

**FABRICATION AND CHARACTERIZATION OF GROUP II-VI
SEMICONDUCTOR THIN FILMS**



Defining futures

By

MUHAMMAD UMER FAROOQ

(2009-NUST-MS PhD-MS-E-08)

Department of Materials Engineering

School of Chemical and Materials Engineering

National University of Sciences and Technology

(NUST),

Islamabad, Pakistan

School of Chemical and Materials Engineering
National University of Sciences and Technology (NUST), H-12,
Islamabad, Pakistan

Certificate

This is to certify that the work in this dissertation has been carried out by Muhammad Umer Farooq and completed under my supervision at Thermal Transport Laboratory, School of Chemical and Materials Engineering, National University of Sciences and Technology, Islamabad, Pakistan

Prof. Dr. Asghari Maqsood (SI)

Supervisor

*Thermal Transport Laboratory,
Department of Materials Engineering*

*School of Chemical and Materials Engineering,
National University of Sciences and Technology,
Islamabad, Pakistan*

Submitted through

Prof. Dr. M. Shahid

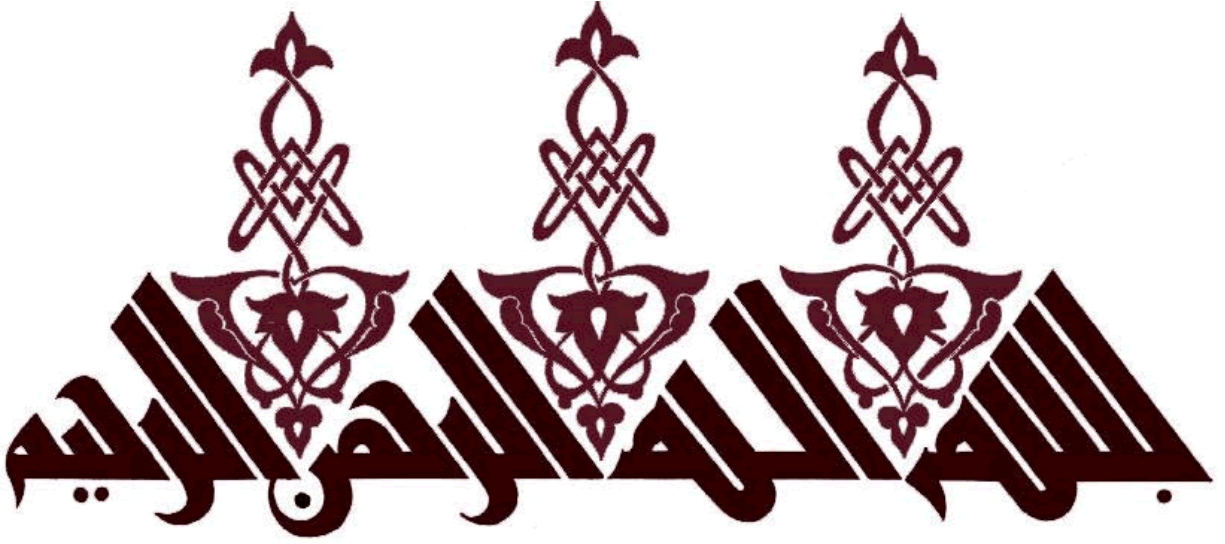
(HoD)

*Department of Materials Engineering
School of Chemical and Materials Engineering,
National University of Sciences and Technology,
Islamabad, Pakistan*

Dr. N.A. Shah

Co-Supervisor

*Department of Physics,
COMSATS Institute of Information
Technology, Islamabad, Pakistan*



وَبِإِسْمِ اللَّهِ الرَّحْمَنِ الرَّحِيمِ

Acknowledgements

All the admiration for Almighty Allah who is the creator of the universe and has the complete knowledge about each and every thing in this universe which exist and which will exist in the future and Who enable d me to seek a little from His absolute knowledge. And He delivered His messages by the Holy Prophet PBUH, Who was the teacher of all mankind. I testify that there is no deity worthy of being worshiped except Allah. He is one and has no partner. I equally testify that Muhammad PBUH is His Messenger.

I wish to thank my supervisor Meritorious Prof. Dr. Asghari Maqsood (Sitara-e-Imtiaz) for all of her support, advice and guidance. I would also like to thank my co-supervisor, Dr. Nazar Abbas Shah who guided and facilitated me a lot while doing experimental work in his laboratory.

I am also grateful to Dr. Muhammad Mujahid, the Principal of SCME for giving permission to work with full liberty even after working hours. I am thankful to Prof. Dr. Muhammad Shahid, HoD Materials Department, for providing access to departmental facilities. I am extremely thankful to my seniors, Sajid Butt and Aftab Ikram and Ahmad Faraz for guiding and encouraging me to do my work. I strongly acknowledge Mr. Waqar Mahmood who helped me in fabrication and optical characterization of materials. Thanks also to Mr. Ali Abbas for helping me in optical characterization. I am very thankful to my class fellows specially Mr. Shahid Ameer, Mr. Mujtaba Ikram, Majid Khan, Shehzad Salam and Asif Mahmood for their great help affection and love. I will always remember the assistance of Mr. Shams, SEM and Mr. Zafar, TTL Laboratory SCME while working during my research. I would like to thanks my fiancé Qurat-UI-Aain for her encouragement. I am also highly thankful to Ms. Tabassum, for her encouragement and cooperation.

I am thankful to my all room-mates, especially to Mr. Nasir Mahmood and Mr. Shahzad Azad for their company and patience during research days. I have no words to describe my sensation of respect about my family, who remembered me in their prayers. Perhaps without their shadow of love; it would never possible for me to attain this target. May Allah bless them with health, wealth, happiness and faith.

Muhammad Umer Farooq

DEDICATED TO

My beloved parents and my dear brother, M. Akmal Farooq

May Allah bless them,

and

My loving family who always prayed for me

Table of Contents

Chapter 1.....	12
1.1 Vacuum	12
1.2 Types of Vacuum Pumps.....	12
1.2.1 Vapor-stream pumps	13
1.2.2 Mechanical pumps	13
1.2.3 Chemical pumps.....	13
1.2.4 Sorption pumps	13
1.2.5 Cryo-pumps.....	13
1.3 Vacuum Gauge.....	14
1.4 What is Thin Film.....	14
1.5 Fabrication Techniques	14
1.5.1 Chemical Vapor Deposition (CVD)	15
1.5.2 Physical Vapor Deposition (PVD)	15
1.6 Vapor Sources	16
1.7 Adhesion of Thin Films.....	16
1.7.1 Chemical Adhesion.....	16
1.7.2 Dispersive Adhesion	17
1.8 Substrates	17
1.9 Atomic Picture of Substrate and Film Growth	17
1.10 Semiconductor Materials.....	19
1.11 Applications of Optical Coatings	20
1.12 Close Space Sublimation Technique	20
1.12.1 Advantages Over Others Fabricating Techniques.....	20
1.12.2 Fabrication Procedure	21
1.12.3 Functioning of Different Components	22
1.12.4 Limitations of Close Space Sublimation Apparatus	23
1.13 References	23
Chapter 2.....	24
2.1 II-VI Semiconductors	24
2.2 ZnTe Thin Film	25

2.2.1	Basic Properties of ZnTe.....	25
2.2.2	Fabrication of ZnTe	25
2.2.3	Structural properties.....	26
2.2.4	Electrical Properties	27
2.2.5	Optical Properties.....	27
2.3	Zinc Selenide(ZnSe).....	28
2.4	GaSe (Gallium Selenide) crystals.....	28
	References	29
	Chapter 3.....	31
3.1	Structural Properties.....	31
3.1.1	X-Ray Diffraction	31
3.1.2	Bragg's law	31
3.1.3	Crystallite Size	32
3.2	Morphology and elemental compositional.....	33
3.2.1	Scanning Electron Microscopy (SEM)	33
3.2.2	EDX Analysis	34
3.2.3	Atomic Force Microscopy (AFM)	35
3.3	Optical characterization.....	36
3.3.1	Spectrophotometer	36
3.4	Electrical Characterization	38
3.4.1	Two-probe method.....	38
3.4.2	The Hall Effect.....	39
3.4.3	Van Der Pauw Method.....	40
3.5	Characteristics Resistances via Van der Pauw technique:.....	41
3.5.1	Sheet Resistance.....	41
3.5.2	Sheet Density	41
3.5.3	Hall mobility	43
	References	43
	Chapter 4.....	45
4.2	Structural Analysis.....	45
4.3	Surface Morphology.....	47
4.4	Compositional Analysis	51

4.5 Morphological Study	53
Chapter 5.....	56
5.1 General Electrical Properties of ZnTe Films	56
5.2 Hall Effect Measurement System (HMS-5000)	56
5.2.1 Hall coefficient of ZnTe thin films	57
5.2.2 Mobility and concentration for ZnTe thin films	58
5.2.3 Resistivity measurements using van der pauw technique for ZnTe films.....	61
5.2.4 Conductivity for ZnTe thin films	63
5.2.5 Sheet magneto-resistance for ZnTe thin films	65
References	67
Chapter6	68
6.1 Optical Analysis	68
6.1.1 Calculation of Band Gap, Refractive Index and Thickness	68
6.2 Comparison of As deposited and Annealed ZnTe.....	70
6.3 Copper Doping Effect.....	72
6.4 Silver Doping Effect.....	73
References:	77
Conclusions	78
Future work.....	79

List of Figures and Tables

Figure 1. 1 Idealized schematic of substrate during initial stages of deposition.	18
Figure 1. 2: Schematic cross section of poly crystalline thin film grown on amorphous substrate	19
Figure 1. 3 :CSS Apparatus Developed at Thermal Transport Laboratory, SCME, NUST	22
Figure 2. 1: Zincblende (Cubic)Crystal Structure of ZnTe.....	26
Figure 3. 1: Interplanar distance and glancing angle.....	32
Figure 3. 2: The using of diffraction curve to determine the particle size	32
Figure 3. 3 :Schematic Diagram of SEM.....	34
Figure 3. 4: Block diagram of AFM operation.	36
Figure 3. 5: Transmission spectrum to measure the thickness and refractive index.....	37
Figure 3. 6: Schematic of Spectrophotometer for transmittance.	38
Figure 3. 7: Keithley 4200-SCS for Electrical Characterization	39
Figure 3. 8: Schematic diagram of the Hall Effect.	40
Figure 4. 1: XRD pattern for ZnTe samples.....	46
Figure 4. 2: SEM image at lower Resolution.....	48
Figure 4. 3:SEM image at high Resolution.....	48
Figure 4. 4: Effect of Temperature on Microstructure.....	49
Figure 4. 5: Effect of temperature on Microstructure.....	49
Figure 4. 6: Microstructure of Ag Doped ZnTe at lower magnification	50
Figure 4. 7: Microstructure of Ag Doped ZnTe at higher magnification	50
Figure 4. 8: Micrographs of Cu Doped ZnTe at low resolution	51
Figure 4. 9: Micrographs of Cu Doped ZnTe at high resolution	51
Figure 4.10: AFM images of ZnTe thin films (a) as deposited (b) annealed at 380 ⁰ C for 1 hour.	53
Figure 4. 11: Morphology of Ag(20 min doped) annealed at 380 ⁰ C for 1hour.....	54
Figure 4. 12: Morphology of Cu (10min doped) doped ZnTe and annealed at 380 ⁰ C.....	54
Figure 5. 1: Bulk Concentration for as deposited ZnTe and Ag Doped ZnTe samples.....	58
Figure 5. 2: Bulk Concentration for as deposited ZnTe and Cu doped ZnTe samples.....	59
Figure 5. 3: Sheet Concentration for as deposited ZnTe and Ag doped ZnTe samples	59
Figure 5. 4: Sheet Concentration for as deposited ZnTe and Cu doped ZnTe samples.....	60
Figure 5. 5: Mobility variations for as deposited ZnTe and Cu doped ZnTe	60
Figure 5. 6: Mobility variations for as deposited ZnTe and Ag doped ZnTe samples	60

Figure 5. 7: Change in resistivity for as deposited ZnTe and Cu doped ZnTe	62
Figure 5. 8: Change in resistivity for as deposited ZnTe and Ag doped ZnTe.....	62
Figure 5. 9: Conductivity comparison for as deposited ZnTe and Cu doped ZnTe samples.....	64
Figure 5. 10: Conductivity comparison for as deposited ZnTe and Ag doped ZnTe samples	64
Figure 5. 11: Magneto-resistance variations for as deposited and Ag/Cu doped samples	66
Table 2. 1: Basic Properties of ZnTe films	25
Table 5. 1: Nature of Material and type of charge carrier	57
Table 5. 2: Sheet concentration, bulk concentration and mobility for as deposited and doped ZnTe films.....	61
Table 5. 3: Resistivity for ZnTe films.....	63
Table 5. 4: Conductivity for ZnTe films	65
Table 5. 5: Magneto-resistance for as deposited and doped ZnTe samples.....	66
Table 6.1: Optical Band Gaps of Ag Doped	76
Table 6.2: Optical Band Gaps of Ag Doped	76
Table 6.3: Refractive Indices.....	77

Abstract

ZnTe thin films were fabricated using Close Space Sublimation (CSS) technique. ZnTe films (as deposited, annealed and doped) were fabricated under vacuum on transparent glass slides. Structural, morphological, optical and electrical properties of ZnTe films were studied before and after annealing. The structure and morphology of the films were studied by XRD, SEM and the composition of the films was analyzed by EDX. Electrical characterization was done by the Hall Effect Measurement System. By this apparatus resistivity, mobility, sheet concentration, type of semiconductor (p or n type), bulk concentration and magneto-resistance were measured. Optical characterization was carried out by UV-Spectrophotometer. For all the fabricated films the various optical parameters e.g. thickness, transmission and band gap were calculated.

The main purpose of this research was to improve the electrical properties and optical properties e.g. electrical conductivity, mobility, sheet resistance/concentration, band gap etc. of the fabricated thin films through CSS. The doping of various elements such as Ag and Cu was performed to observe their effects on morphology, structure, electrical and photovoltaic properties of the parent material due to their specific nature (n or p type) and as a function of various evaporation times of the doping elements. The evaporation of Ag and Cu was performed for different times under same annealing temperature and vacuum conditions. It was observed that electrical and optical properties of the fabricated films enhanced with dopant type and annealing temperature.

Chapter 1

Introduction

1.1 Vacuum

Vacuum is defined as a space which characterized without any matter. In practical sense, it is defined as a space with traces of matter. With reduction of pressure of the corresponding gas in enclosure is helpful in achieving vacuum. Approach to perfect vacuum is related to the quality of that partial vacuum that refers to it. By considering other parameters as constant, high quality vacuum means lower pressure of gas. According practical point of view, Vacuums science is a significant and convincing field in today's scientific era.

Following purposes are utilized in the vacuum science:

- Avoiding of collisions
- Removal of dissolved gases
- Reduction in the transfer of energy
- Production of free surfaces (Contaminated)
- Decrease in boiling points of the material

For deposition of thin films, vacuum is used in the technique of Closed Space Sublimation to obtain such appropriate purposes.

1.2 Types of Vacuum Pumps

Vacuum pumps are of various types and are used to achieve vacuum in a vessel of particular shape. Accordance of the working principle, vacuum pumps is divided into two main groups:

- i. The pumped volume removes the gas particles and discharges these to the atmospheric Environment at one or more stages of compression.
- ii. Removal of chemically binded particles at a solid wall, which is often, characterized as a part of that boundary of the volume which being pumped at a stage.

Major types of pumps according to their working principle are as follows

1.2.1 Vapor-stream pumps.

This type describe pumps in which the molecules of gas to be pumped out are caused to move forward in the direction of desired orientation by contact with heavy molecules of pump fluid vapor, which cause to derive their velocity by boiling effect from a response of a liquid reservoir. In other words, a mechanical pump is that which backs the vapor-stream pumps.

1.2.2 Mechanical pumps

Mechanical pumps are those in which gas is trapped, compressed and then removed from one specific direction to other direction i.e. from low pressure to high pressure sides of that specific pump, where it is subjected in form of expel to the environment atmosphere either using directly or through second mechanical pump which is “backing” pump.

1.2.3 Chemical pumps

Chemical pumps are those in which molecules are to be withdrawn from the workings chamber and then these are caused to accumulate chemically with characteristics of highly reactive substances for example titanium thus this being converted to and then trapped in the solid phase region. Using sputtering or with help of evaporator, these getters are dispersed on the surfaces of pumps.

1.2.4 Sorption pumps

Sorption pumps are characterized in which the molecules that are to be pumped out and then these are absorbed physically. These can be absorbed physically using Van der Waal forces on prepared substances for specific area of large dimensions e.g. in case of zeolites or charcoal. By cooling, the sorption can be aided and then keep the sorbent below temperature at room conditions.

1.2.5 Cryo-pumps

Cryo pumps are those using vessels with characteristics of metal surfaces with chemically non-reactive internal behavior, and these are cooled using refrigerants which cause to condense of these gases which is to be pumped out. In our close space sublimation apparatus, rotary Van pump is used. Its ranges from 10^3 mbar to 10^{-3} mbar.

1.3 Vacuum Gauge

The device which is used for measurement of the pressure is termed as vacuum gauge. Many gauges are used for the purpose of measurement of the pressure. Ranges of the gauge describe the type of gauge. In our apparatus of Closed Space Sublimation, Pirani gauge can be used to measure pressure with range till up to 10^3 mbar.

1.4 What is Thin Film

Film characterized as fine layers of material which are formed by the process of the random nucleation and then as a result of growth processes of these individually reacting atomic, condensing or reacting ionic, molecular species on a substrate. The chemical, physical and structural properties of these thin films depend on different deposition parameters and also depend on thickness of the films. Types of chemical species with which they comprise describe basically the properties of thin films. Microstructure, surface morphology, chemical composition, homogeneity and purity tell about the electrical, mechanical and optical behavior of thin films. These all properties are strongly dependent on the type of fabrication method of films, parameters, and treatments for post-deposition conditions. The material which is taken as thin film shows different features of characteristics moderately in form of bulk such as electrical, optical, magnetic, mechanical and thermal. Difference in the characteristics of these thin film accordance with bulk form is of larger surface to volume ratio. Thin films properties become affected with properties of the interface and surface of the substrate because of the effect of nucleation phenomenon, adsorbed gases, surface mobility, contamination, surface topography, crystallographic orientation and thermal mismatches [1].

1.5 Fabrication Techniques

Thin films can be produced using different fabrication techniques. There are many advantages and disadvantages for every technique. Optimization for a technique should be necessary to acquiesce properties of our own desire. Deposition techniques for thin films are divided as [2-4]:

1. Physical Vapor Deposition (PVD)
2. Chemical Vapor Deposition (CVD)
3. Electrolysis or Solution Growth
4. Electro-Chemical Deposition (ECD)

From above four techniques, The CVD and PVD are described as.

1.5.1 Chemical Vapor Deposition (CVD)

Chemical vapor deposition is a process that involves the reaction of gaseous reactants to give solid as a product. Two types of CVD are as follows,

1. Thermal decomposition of a gas which result to form solid as product.
2. Two or more species in chemical reaction.

In industry, these types are often used to generate compound of semiconductors and of ceramics material.

1.5.2 Physical Vapor Deposition (PVD)

PVD is a process that is defined as in which transferring growth species from a target or source and then it deposit on a substrate which favors the formation of a thin film. This process actually proceeds and mostly this process does not involve any reactions of chemical type. For removal of the growth species from target or source, various methods are investigated. The thickness of the deposits can be varying i.e. ranges from angstroms level to millimeters level.

These methods are generally divided as:

1. Sputtering
2. Evaporation

1.5.2.1 Sputtering

Sputtering is a process that relies on plasma which is used to knock material from a target at rate as few atoms at a time span. Plasma is usually taken a noble gas for example Argon. At low temperature, the target should be kept, as the process is not one of evaporation method, so as a consequence making this one of the reliable and flexible techniques for depositions of thin films. It is extremely beneficial for mixtures or compounds, where different types of components will tend to evaporate at variable rates [5-6].

1.5.2.2 Evaporation

Molecules or Atoms are liberate using heating from every material that is in its phase of liquid or solid and as a result of it that in the closed system a certain pressure which is equilibrium pressure, which is often called the vapor pressure of saturation and that is established at a given value of temperature.

1.6 Vapor Sources

In a vacuum system, the evaporation for materials requires a vapor and then to provide the heat of vaporization while condition is maintaining the charge at a suitable temperature which is sufficiently high enough to provide the vapor pressure (desired).

Using an electric resistance heater, thermal evaporator is to melt the required material and as a result it increases vapor pressure to a certain specific useful range. Actually this should be done at a high vacuum, which favor as it allow enough vapor to approximate the substrate level without any reaction or scattering against the atoms of gas-phase in chamber, and to do reduction in the incorporation of impurities as the incorporation of impurities reduces from the gas of the residual which is in the vacuum chamber.

High energy beam is fired from an evaporator of electron beam which come from an electron gun which result in boiling of a small slit of the material; as the heating is not constant or uniform, deposition of materials with characteristics of lower vapor pressure is happened. Using ablation process, pulsed laser deposition systems works. Conversion of plasma is occur when Pulse of laser light which is focused vaporize the target material's surface. This plasma is usually characterized as it reverts to the gas before it approaches the substrate [7].

1.7 Adhesion of Thin Films

The adhesion of thin films to a substrate is a significant feature. Strengthen and nature of binding forces between the substrate and the film is an important factor [8]. A couple of major types of adhesion process are discussed here:

1.7.1 Chemical Adhesion

Two different types of materials may form a compound where they join. Joint of two types are most chemically occur. Ionic bonding favor the stronger one in which atoms of two different materials usually swap or in case of covalent bonding, it usually share outer electrons. Hydrogen bonding is of weaker type like a weaker bond is mostly formed if the atoms of different elements like oxygen, nitrogen, fluorine are present and from which atoms of two materials usually share a nucleus of hydrogen.

1.7.2 Dispersive Adhesion

Adhesion can be because of the van der Waal forces which are identified as dispersive adsorption or adhesion. When positively and negatively charged ends of two molecules are attracted then as a result, the Van der Waal's force is developed. The strength of the adhesion between substrate and thin film depends on which of the above mechanisms occur between the two, and the surface area over which they become in contact. Scotch tape test is used for a qualitative guess for degree of adhesion, in which using adhesive tape; the film to be tested is lifted off the substrate. Different techniques for film abrasion are often used, their results being totally dependent on the film's hardness [8]. Sticking coefficient is defined as the ratio between the rate of adsorption to the rate, at which the adsorptive species reaches at the total surface, i.e., covered and uncovered. Sticking coefficient is a function of temperature, surface coverage and the surface morphology. Using scotch tape test, degree of adhesion is estimated, in which in other words, the film is lifted off from the substrate using adhesive tape.

1.8 Substrates

Substrates are taken as mechanical support for the deposited film. In different sort of applications, substrates can also serve in different ways, like in case of electronic applications, substrates of semi-conductor thin films serve as an insulator. If we desire to increase the life of thin films and to maintain proper properties of thin film for a long span of time then we have to use such a substrate with such properties in which substrate should not react with thin film deposited. Certain requirements should be fulfilling for substrates regarding with characteristics of adhesion and stability even for different changeable conditions like in case of higher temperature. These variable conditions may occur during fabrication of thin films as well as where these are to be used further. To maintain surface evenly heated, appropriate thermal conductivity is required. Substrate surface is selected as flat and smooth to fabricate or produce thin films with desired required parameters.

1.9 Atomic Picture of Substrate and Film Growth

During growth of thin films, an idealized picture of a surface of substrate at atomic level is as shown in below Figure 1.1. When some atoms reach at surface of substrate then these atoms have 2nd degree of freedom. Atoms at the steps which are characterized as first degree of

freedom or in other words at kinks have, on the average, less energy than those which are characterized with the flat surface. Reduction in energy to the substrate while striking the surface, as a consequence of it, on the surface mobility of these atoms also decreases. The main need of substrate temperature (at elevated condition) is to generate enough sufficient energy for atoms so that they can make necessary suitable movements for the accommodation at the substrate and among themselves [9].

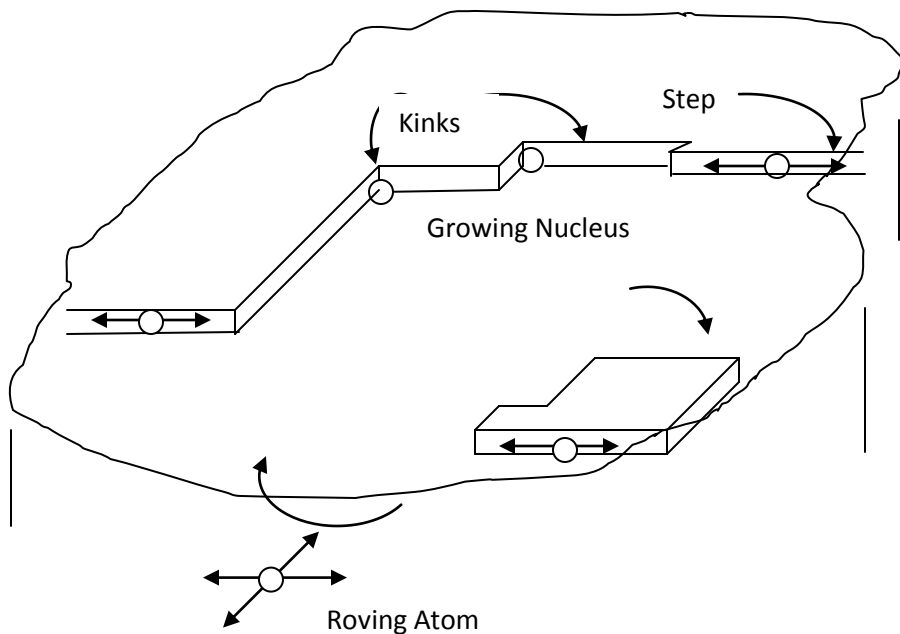


Figure 1.1 Idealized schematic of substrate during initial stages of deposition.

Portion of the film which is nearby the substrate usually most disordered, this is where lattice matches and impurity defects are accommodated as also shown in below Figure 1.2.

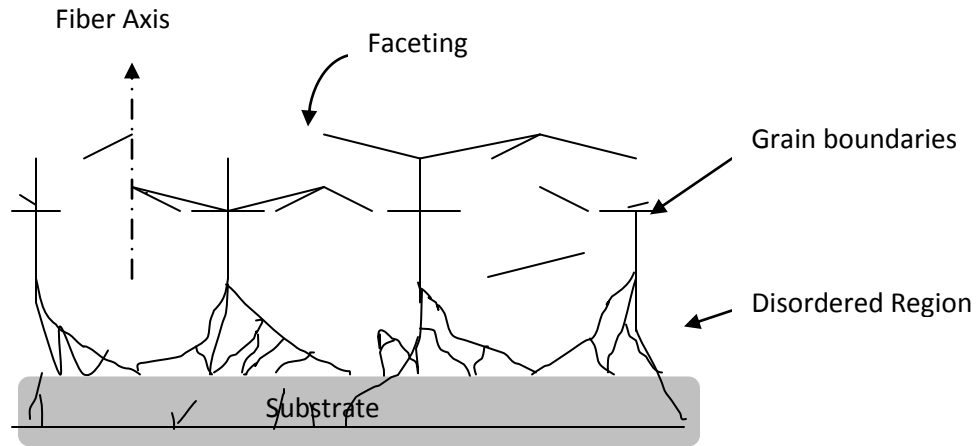


Figure1.2: Schematic of cross section of poly crystalline thin film grown on amorphous substrate [9].

As thickness of film increases during growth process, faceting occurs on various grains due to difference in growth rates of various crystals. Crystallites which are big enough grow at expense of smaller ones and give us fibrous like texture. In the end, texture of film is of order of grain dimension because of faceting phenomenon [8].

1.10 Semiconductor Materials

Semiconductor is a substance whose electrical properties can be modified by various factors. These materials have electrical characteristics between the conductor and insulator materials. Electrical conductivity reaches as high as metal at temperature rises and reaches as low as insulator as temperature decreases. From band theory, semiconductors are defined as those materials having conduction band and valence band being partially filled at room temperature and very small energy gap (nearly 1 eV) between these two bands.

Semiconductor materials can be doped to change their electrical properties for various applications. Each year various new methods are developed for semiconductor application and various doping mechanisms are studied. These are normally classified

- 1) Elemental and
- 2) Compound semiconductors.

Any semiconductor substance comprises two or more materials, like from I and III groups or II and VI groups of periodic table are named as compound semiconductor.

1.11 Applications of Optical Coatings

Optical coatings have numerous applications ranging from antireflection coatings to laser optics, from interference filters on solar panels to plate glass infrared solar reflectors. In the synthesis of optical filters, thin films having gradient refractive indexes are deposited on pre-forms which are used to draw optical fibers. In such process, dielectric substances with predefined absorption indices and refraction coefficients are needed. In order to increase the intensity of luminous flux, Ir coatings are used. Laser optics deploy metallic reflective coatings, which are highly resistant to degradation in high radiation intensities.

- Thin coatings of magnetic materials have vast applications ranging from data storage to control systems as well as memory devices. These substrates can be glasses, metals or polymeric.
- Thin films have ever rising industrial usage for optical storage devices in computer memory chips and compact hard disks. Various techniques for the deposition of organic polymer layers as storage options and also protective coatings.

1.12 Close Space Sublimation Technique

Close space sublimation is a simple technique of film fabrication and this setup was built at our department by my senior student Sajid Butt at Thermal Transport Lab at SCME, NUST and I brought some modification and improvement in this apparatus.

1.12.1 Advantages Over Others Fabricating Techniques

This method of fabrication is very easy. The film obtained by this method having very low surface roughness (which was calculated by atomic forced microscopy and is discussed in next chapter). The deposition rate is very high as compared to other fabricating techniques. Because of under vacuum fabrication, the films grown are free from the impurities and extra species which may react in the open atmosphere.

The advantages over other techniques are that, it has high transport rate under very low pressure up to 10^6 mbar. The temperature is also kept moderate. The process is done by the condensation of the vapors of the material on the substrate which is placed very close to the source.

There is less wastage of material as compared to other fabricating techniques because the source and substrate are separated by a very thin mica sheet, so the vapors are directly kept to closed space. The films formed by this technique having good crystallographic orientation and show good opto-electrical properties for photo voltaic applications.

1.12.2 Fabrication Procedure

The material which is to be deposited must be highly pure as pure powder having low temperature of sublimation & materials used in deposition apparatus can be in only powder form. Powder is kept in a graphite boat and substrate (may be glass or other) is kept in a mica sheet. The distance between source and substrate is taken as minimum as possible because uniformity of the film depends on the distance between the source and substrate. With the help of rotary pump, the pressure in the chamber must be reduced till the possible limit which is in the order of 10^{-2} to 10^{-3} mbar. After that the substrate temperature is raised till the sublimation temperature. The source temperature must be taken lower than substrate temperature because vapors may travel from source to substrate. When the sublimation is started, the film is deposited for the given time of your own choice because deposition time may influence on the thickness of the growing thin film.

The Close Space Sublimation apparatus develop at SCME is shown in figure given below with different parts.

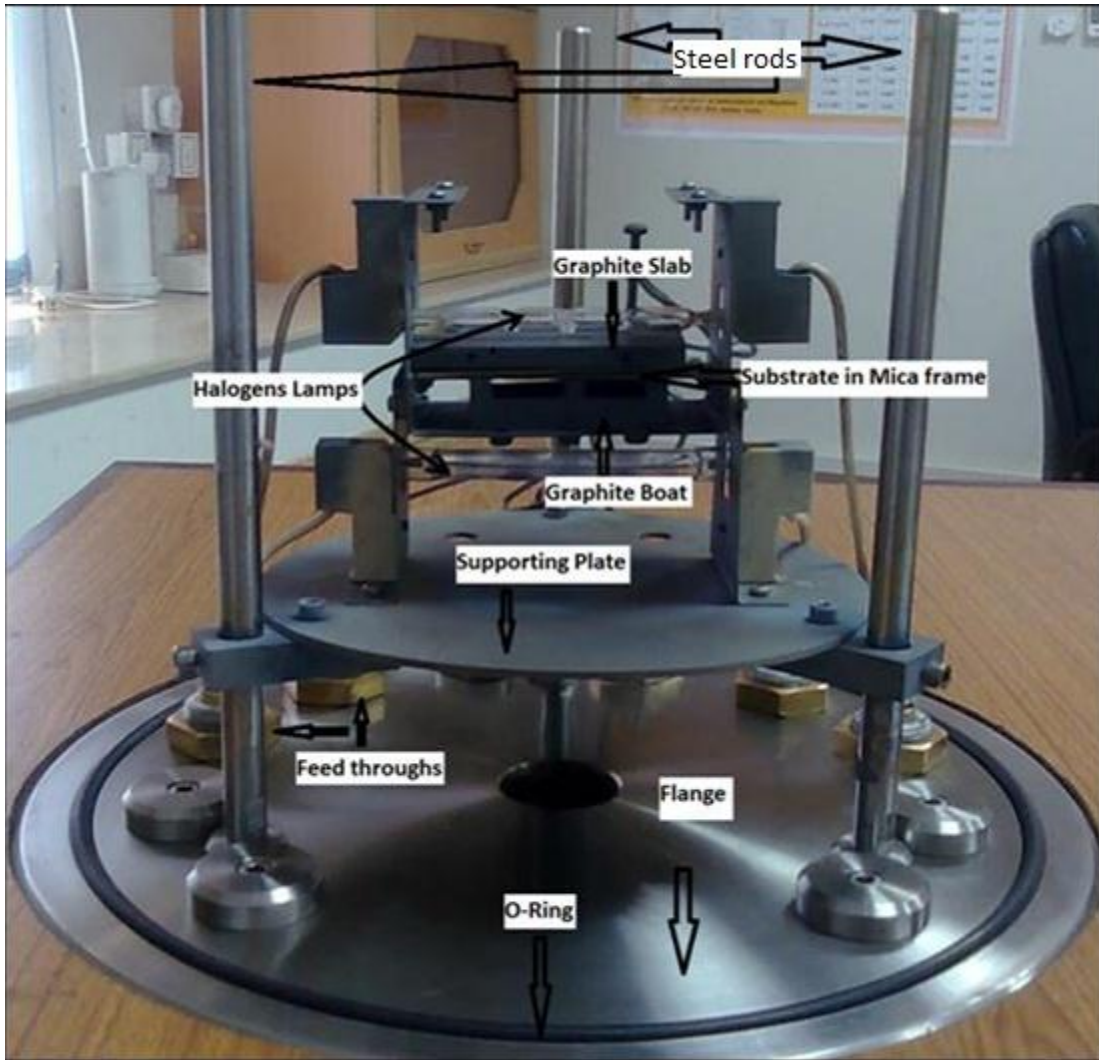


Figure 1.3 :CSS Apparatus Developed at Thermal Transport Laboratory, SCME, NUST [10]

1.12.3 Functioning of Different Components

The vacuum chamber contain Stainless Steel vertical jar. A circular flange was used to mount the other assembly on it. Supporting steel was fitted on rods to mount source, substrate and heating lambs. Graphite was used to hold the source material. Two halogen lambs 1000Watts and 500Watts are used to heat source material placed in graphite boat and substrate placed in mica frame, covered with a graphite slab respectively. Graphite slab is used to heat the substrate uniformly. Mica acts as a thermal insulator between source and substrate. Two temperature controllers, one for source and other for substrate was used to control temperature

A rotary vacuum pump was attached to the chamber to decrease the pressure inside the chamber. The range of this rotary pump is till 10^{-3} mbar. This pressure may reduce more than this limit by using diffusion pump which may take the pressure till 10^{-6} mbar.

PIRANI gauge is used to measure the pressure of the chamber. This gauge can read the pressure in the range of 10^3 to 10^{-3} .

1.12.4 Limitations of Close Space Sublimation Apparatus

This technique is only for those materials who are in powder form and having low sublimation temperature because the material that having higher temperature are not sublimed hence not evaporate and may not be deposited. The temperature limit is of 1000°C . Also the thickness of the film may not be controlled. We cannot get the film of required thickness.

1.13 References

- [1] K. Sheshan, Hand Book of Thin Film Deposition Processes and Techniques, Intel corporation, California (2000).
- [2] M. Ohring, *The Materials Science, of Thin Films*, **Academic Press**, San Diego, New York, Boston, London, Sydney, Tokyo, Toronto, (2002).
- [3] L. Eckertova, *Physics of Thin Films*, Plenum Press, New York, (1977).
- [4] K. L. Chopra and S. R. Das, *Thin Film Solar Cells*, Plenum Press, New York (1983).
- [5] G. Cao, *NanoStructures and NanoMaterials*, Imperial College Press, (2004).
- [6] A. Ali, "Fabrication and Characterization of two sourced evaporated Cd-based II-VI thin films"
- [7] A. Ali, "Fabrication and Characterization of two sourced evaporated Cd-based II-VI thin films"
- [8] L. Eckertová, *Physics of Thin Films*, Plenum Press, New York, (1977).
- [9] A. L. Fahrenbrach, R. H. Bube, *Fundamental of Solar Cells*, Academic Press, Inc. New York (1983).
- [10] S. Butt, MS thesis, TTL laboratory, SCME, NUST

Chapter 2

Properties of II-VI Semiconductors Materials

2.1 II-VI Semiconductors

These semiconductors are based on one atomic element from Group II and one atomic element from Group VI. Representative II-VI semiconductors are ZnS, ZnSe and ZnTe (zinc blende lattice structure); CdS and CdSe, (zinc blende or the wurtzite lattice structure) and CdTe which forms in the wurtzite lattice structure. Wide band gap II–VI compounds are been applied to optoelectronic devices, especially light-emitting devices in the short-wavelength region of visible light, because of their direct gap and suitable band gap energies semiconductors and have higher melting points.

Binary and ternary ii-iv compound present wide range of optical and electrical properties. Due to these properties, they become important class of material becomes competing candidates for silicon and other semiconductor. The wide band gap compound of ii-iv semiconductor ZnTe with direct band gap of 2.26eV at room temperature is excellent material for optoelectronic device in the visible region of electromagnetic spectra.[1-2]

Mostly these compound materials are in the form of films. The thickness of the film can be varied from micron to Nano scale and shows different properties. The properties of these films depends upon the certain parameters like thickness of the film, temperature and method of film deposition.

Now we will discuss these properties in detail.

2.2 ZnTe Thin Film

2.2.1 Basic Properties of ZnTe

The basic properties of ZnTe are given below.

Table 2. 1: Basic Properties of ZnTe films [3]

Formula	ZnTe
Color	Red Crystal, Red powder
Odor	No
Melting Point	1238.5°C
Toxicity	Non Toxic
Molecular Weight	193.01 g/mol
Density	634 g/cm ³
Crystal Structure	Zincblende (cubic)
Solubility in water	Decomposes

2.2.2 Fabrication of ZnTe

ZnTe has been prepared in laboratory by different techniques including thermal evaporation, chemical bath deposition, molecular beam epitaxy, DC sputtering, RF sputtering etc. We have fabricated ZnTe by using Close Space Sublimation technique in which ZnTe in powder form is sublimed on a glass substrate under vacuum. I preferred this fabricating technique because it has many advantages over other fabricating techniques which are discussed in next coming chapter. From this technique, we have studied the properties of ZnTe thin film at different parameters like deposition time and different annealing temperature. By changing these parameters, the optical structural and electrical properties of the given thin films have shown great influence.

After studying the properties of as deposited and annealed thin films, The ZnTe thin films were doped by copper as well as silver using the same technique. The film was doped for different time and after that I studied the properties of that doped thin films.

2.2.3 Structural properties

ZnTe films are cubic in structure (Fig. 1) when it is fabricated by thermal evaporation method. In thermally evaporated films, the crystalline size of poly crystalline ZnTe is effected by temperature of the substrate .The grain size at amorphous substrate range from 25A° at substrate temperature of 150C° to 400A° at 400C° temperature of substrate. In general the at higher temperature and higher deposition rate the better structure is formed.[3-4]. There are varieties of the methods for the preparation of ZnTe films including thermal evaporation [10-11],RF and dc sputtering[12],molecular beam epitaxy (MBE)[13], metal organic phase epitaxy (MOVPE)[14],chemical vapor deposition(CVD)[16,17], electro-deposition[15] and pulsed laser ablation[18].

The ZnTe films shows mixed structure cubic as well as hexagonal phases of compound. ZnTe films could be obtained by electro-deposition method.

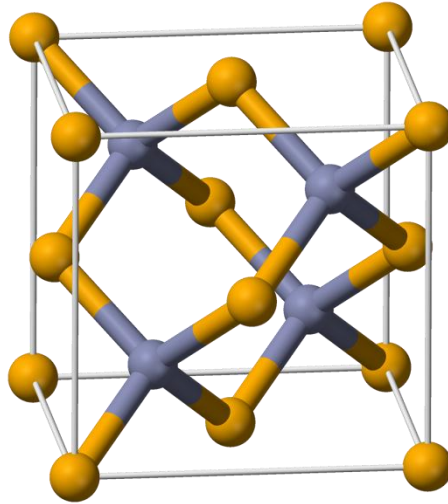


Figure 2. 1: Zincblende (Cubic)Crystal Structure of ZnTe [3]

2.2.4 Electrical Properties

ZnTe is a highly resistive P-type semiconductor compound and in ZnTe thin films, the resistivity in the range 10^5 to $10^7 \Omega\text{-cm}$ [5,6,7]. The resistivities of such films could be reduced in case of non-stoichiometric ZnTe films and also decreasing of conductivity with increasing the thickness was observed in case of ion beam sputtering[8]. ZnSe films deposited by vacuum evaporation have a high resistivity ($>5 \times 10^8 \Omega\text{-cm}$). High conductivity was obtained by annealing them in the Zn vapors at 500°C , the final lateral resistivity of ZnSe films deposited on glass substrate ranged from $0.5 \Omega\text{-cm}$ for a film thickness of $0.3 \mu\text{m}$ to $40 \Omega\text{-cm}$ for film thickness of $1.8 \mu\text{m}$, showing a correlation between film thickness and final resistivity, electron density of 10^{19}cm^{-3} and corresponding mobility $3.5 \times 10^{-2} \text{cm}^2 \text{V}^{-1} \text{s}^{-1}$ were obtained[17]. ZnSe films grown by MBE and doped with Li to make p-type, the hole entities of order of $1 \times 10^{16} \text{cm}^{-3}$ were measured[18].

2.2.5 Optical Properties

Optical properties of ZnTe depend upon the deposition parameter like thickness of the film, temperature and also for different doping materials. However, in thermally evaporated ZnTe thin films, the optical direct band gap would be 2.23eV at room temperature and 2.24eV at 325°C . [9] When thickness of the films ($\sim 12 \mu\text{m}$) by hot wall evaporation, energy gap was 2.25eV . [4] Refractive index of the ZnTe thin films at room temperature depend upon the film thickness in case of thermally evaporated. For ZnTe films by RF-sputtering [22] energy gap was 2.26eV and the long wavelength refractive index n increased with RF power from 2.5 to 2.65 for RF power from 200 W to 300 W. Shifting of the band gap due to doping was reported. In case of vacuum evaporated Cu-doped ZnTe films, the undoped films show a sharper absorption edge than Cu-doped films and shifting to lower energy (2.15eV for 7% Cu concentration) [21]. In doping the band gap of the ZnTe can be shift, In case of Cu doped ZnTe films less sharper absorption edges as compared to the un-doped films and shifting to lower energy 2.15eV for 7% Cu concentration [19]. This behavior have also been seen in Cu doped by electro-deposition [18] and band gap also shift for Sb doped thin films[20]. In the case of semiconductor nanocrystals, the effect of the size on the optical properties of the particles is very interesting. Consider a Group II-IV semiconductor, cadmium selenide (CdSe). A 2 nm sized CdSe crystal has blue color fluorescence whereas a larger nanocrystal of CdSe of about 6 nm has

a dark red fluorescence. In order to understand the size dependent optical properties of semiconductor nanoparticles, it is important to know the physics behind what is happening at the nano level.

2.3 Zinc Selenide(ZnSe)

Zinc Selenide is an attractive II-VI semiconducting material having a large band gap of 2.7 eV at room temperature, which attracted considerable attention owing to its wide applications in laser diodes, green-blue light-emitting diodes and solar cells [1]. ZnSe is also a promising material for windows, lenses, output couplers, beam expanders, and optically controlled switching due to its low absorptivity at infrared wavelength, visible transmission and giant photoresistivity [2]. A nanometer-sized semiconductor particle belongs to a state of matter in the transition regions between molecules and solids. From last two-three decades the research on quantum size semiconductor particles has increased enormously due to their exciting novel properties. Now-a-days, semiconductor nanocrystals/nanoparticles are very important materials due to their crystallite/particle size dependent electronic structure, which lead to give tunable electrical as well as optical properties [3–9]. The nanoparticles of ZnSe have been prepared by different methods like sol-gel method, melt quenched method, aqueous colloidal method, reverse miscell method, surfactant-assisted chemistry methods, sonochemical method, solvothermal routes, and vaporphase synthesis [10-13, 14-16] etc. The nanoparticles of many materials already have been synthesized by using microwave rapid heating process using chemical route [17, 18]. Generally, the semiconducting nanoparticles were synthesized by chemical methods and the particle size is controlled by using matrices or ligand shells which also prevents agglomeration of the nanometer size particles. However, these matrices or ligand shells might influence the electronic as well as optical properties of the material therefore it is more favorable to synthesize semiconductor nanoparticles free from these matrices or ligand shells.

2.4 GaSe (Gallium Selenide) crystals

GaSe (Gallium Selenide) crystals used for THz generation shows a large bandwidth of up to 41 THz. **GaSe** is a negative uniaxial layered semiconductor with a hexagonal structure of 62 m point group and a direct bandgap of 2.2 eV at 300 K. GaSe crystal features high damage

threshold, large nonlinear optical coefficient (54 pm/V), suitable transparent range, and low absorption coefficient, which make it an alternative solution for broadband mid infrared electromagnetic waves generation. Due to broadband THz generation and detection using a sub-20 fs laser source, GaSe emitter-detector system performance is considered to achieve comparable or even better results than using thin ZnTe crystals. In order to achieve frequency selective THz wave generation and detection system, GaSe crystals of appropriate thickness should be used.

NOTE: because of material structure it is possible to cleave GaSe crystal along (001) plane only. Another disadvantage is softness and fragility of GaSe.

References

- [1] J.I Cismors , Applied Optics,37(1984)896.
- [2] U.Pal.S.Saha.A.K Chaudhuri ,V.V Rao and H. O Banerjee.j.Phys.Appl.phys.22(1989)965
- [3] Nowshad Amin, Kamaruzzaman Sopian and Makoto Konagai, "Numerical modeling of CdS/CdTe and CdS/CdTe/ZnTe solar cells as a function of CdTe thickness," Solar Energy Materials and Solar Cells, Vol. 91, no. 13, 15 August 2007, pp 1202-1208
- [4] J.B.Webb,D.E.Brodie,Can,Phys.,53(1975)1415.
- [5] Y.Namba,T.Mori,Thin solid Films,39(1976)119.
- [6] H.M.Browm,D.E.Brodie,Can.J.Phys.,50(1972)2512
- [7] S.Kobayashi,N.Saito,T.Shibuya,Jpn.J.App.Phy.,19(1980)1199
- [8] C.J.Moore,B.S.Bharaj,D.E.Brodie,Can.J.Phy.,59(1981)924
- [9] D.A.Gulino,J.Vac.Sci.Technol.,A4(1986)509
- [10] G.K.M.,S.G.Tomlin,J.Phys.D:Appl.Phys.,9(1976)1639
- [11] S.Nam,J.Rhee,B.O.,K.Lee,Y.D.Choi,J.Crystal Growth, 180(1997)47
- [12] R.C.Tu,Y.K.Huang,F.R.Chien,J.Crystal Growth, 180(1997)506.
- [13] H.Bellakhder,F.Debbagh,A.Outzourhit,A.Bennouna,M.Brunel,Solar Energy and Solar cells,45(1997)361.
- [14] T.Baron,K.Saminadayar,S.Tatarenko,J.Crystal Growth,159(1996)271.

- [15] W.kuhn,H.P.Wagnert,H.Stanzi,K.Wolf,S.Lankes,Semicond,Sci.Technol.,6 (1991) 105
- [16] N.B Chaure,J.P.Nair,R.Jayakrishnan,V.Ganesan,R.k.Pandey,Thin Solid films 324 (2001) 447.
- [17] S.Stolyarova,N.Amir,Y.Nemirovsky,J.Crystal Growth,186(1998)55.
- [18] T.Matsumota,T.Ishida,J.Crystal Growth,186(1998)55
- [19] H.Wang,J.Opt.Soc.Am.A,12(4)(1995)769
- [20] S.Ikegami,Solar Cells,23(1988)89.
- [21] S.I Gheyas,S.Hirano,M.Nishio,H.Ogawa,Applied surface Science,100-101(1996)634.
- [22] L.Feng,D.Mao,J.Tang,R.T.Collne,J.U.Trefny,J.Electronic Materials,25(1996)1422.
- [23] H.Bellakhder,A.Outzourhit,E.L.Ameziane,Thin Solid Films,382(2001)30

Chapter 3

Characterization Techniques

This chapter will address the experimental techniques and applications associated with determination of

1. Structural Properties
2. Morphological Properties Elemental Composition
3. Optical Properties
4. Electrical Properties

Characterization was done using X-Ray Diffraction (XRD), Scanning Electron Microscope (SEM), Energy Dispersive X-ray spectroscopy (EDX) and UV-Vis Spectrophotometer. A short description of each technique is given below.

3.1 Structural Properties

3.1.1 X-Ray Diffraction

It is non-destructive technique used to find information about crystallographic planes, phases, unit cell dimension, chemical composition and micro structure of materials [1-4]. Some other structural parameters can also be calculated such as average grain size, particle size, crystallinity, and strain and crystal defects. A typical X-ray diffractometer consist of an x-ray tube, sample holder, and a detector. Monochromatic x-rays are generated from x-ray tube and are directed onto the sample. The sample and detector are rotated continuously and intensity of diffracted x rays is recorded as a function of orientation between samples surface and incident x-ray radiation (2θ). When incident x-rays and the geometry of sample satisfy Bragg's equation ($n\lambda=2d\sin\theta$), constructive interference occurs which lead to a peak. The XRD of pure polymer and nanocomposites was performed in the range of 20-70o using STOE Diffractometer, keeping step size of 0.02o and scan time of 1 s.

3.1.2 Bragg's law

This law has been devised to explain the diffraction phenomenon in crystals. When X-rays come in vicinity of crystal, they are diffracted by parallel planes of crystals which are at equal interplanar spacing. This law is given as under:

$$\lambda = 2 d \sin\theta \dots\dots\dots (1)$$

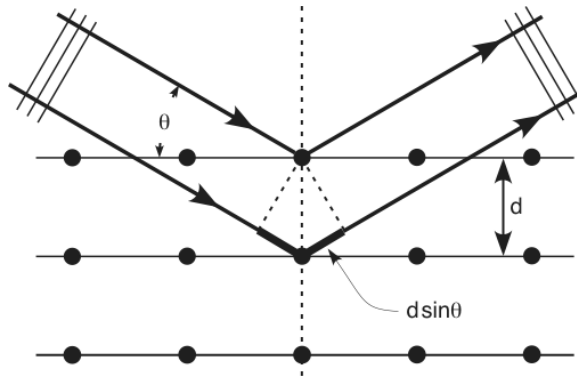


Figure 3.1: Interplanar distance and glancing angle

Where

d = interplanar spacing

θ = Angle between the incident wave and reflected plane.

n = Order of reflection

λ = Wavelength of X-ray

3.1.3 Crystallite Size

Crystallite size/grain size can be estimated using the following relation which takes into account the full width half maximum of the observed peaks, wavelength of incident X-rays and angle of diffraction [5].

$$t = \frac{\lambda}{\beta \cos \theta_{\beta}} \dots\dots\dots (2)$$

In the present work CuK_{α} ($\lambda = 1.5418 \text{ \AA}$) radiations were used for the experiments and the measurements were made at room temperature.

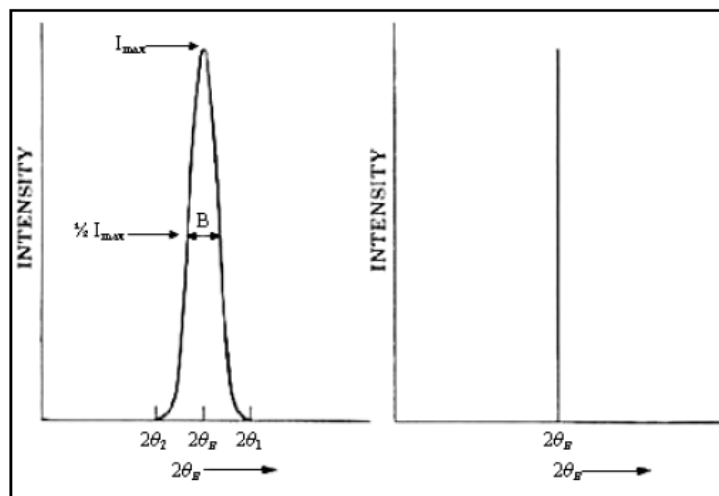


Figure 3.2: The using of diffraction curve to determine the particle size

XRD pattern were obtained by STOE Diffractometer, keeping step size of 0.02° and scan time of 1 s and crystal Structure with phase analysis were carried out on the software STOE installed on the computer attached with XRD machine.

3.2 Morphology and elemental compositional

Morphology of thin films is very important as it directly influences optical and electrical properties. So, proper morphological characterizations were required to work out a morphology with best electrical and optical properties, which was done using SEM and AFM. Elemental composition was also determined using EDX Spectroscopy.

3.2.1 Scanning Electron Microscopy (SEM)

Scanning electron microscopy (SEM) is an imaging technique for material characterization to evaluate micro structural/morphological properties. It can provide important information about the surface features of an object, its texture, the shape, size and arrangement of the particles making up the object. Figure shows a schematic diagram of scanning electron microscopy.

In SEM, electrons are generated from electron gun and are directed onto the sample by using pre-specimen lenses. When the electrons interact with the specimen surface, they are scattered, diffracted or absorbed by specimen. So, there are many processes which occur as a result of interaction of electrons and specimen and generate *backscattered electrons, secondary electrons, X-rays, Auger electrons and photoluminescence electrons*. Of these we were interested in secondary electrons in our present work. The secondary electrons are detected by a scintillation material that produces flashes of light from the electrons. The light flashes are then detected and amplified by a photomultiplier tube. An image can be formed that is strikingly similar to what would be seen through an optical microscope by simply correlating sample scan position with signal [6].

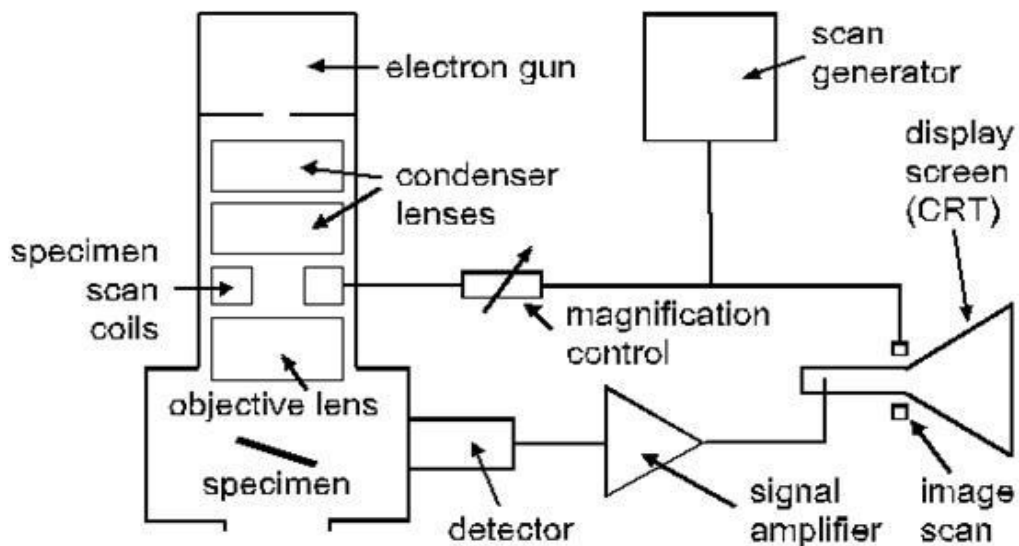


Figure 3.3: Schematic Diagram of SEM

SEM analysis was performed using scanning electron microscope (JSM 6490LA; JEOL) with operating voltage of 20 kV, spot size of 20-60, and a working distance of 10. The images were recorded in SE mode at low and high magnifications. Figure 3.3 shows a schematic of SEM present in School of Chemical and Materials Engineering, National University of Science and Technology, Islamabad.

3.2.2 EDX Analysis

X-rays generated by the interaction of electrons with the specimen may be detected in one of the following two methods.

- Energy Dispersive X-Ray Spectroscopy (EDX or EDS)
- Wavelength Dispersive X-Ray Spectroscopy (WDS).

For identification of elemental composition, energy dispersive X-ray (EDX) spectroscopy is used [7]. When electrons with sufficiently high energy interact with the specimen, they knock off the electrons in the shells of atoms. This causes a vacancy in the orbital of the atom which is filled by the electron in the higher energy shell by radiating some energy and dropping down to the lower energy shell. Such transitions of electrons produce unique amounts of energies for each type of atom which is the key in detecting separate elements and their relevant composition. EDX spectrum gives information that how frequently an X-ray is received for each energy level.

The maxima in EDX spectrum show the elements for which maximum amount of energy has been radiated which indirectly shows its higher concentration. Each peak represents a particular atom which corresponds to a single element. Intensity of peak in spectrum shows the concentration of that element in specimen.

3.2.3 Atomic Force Microscopy (AFM)

Atomic Force Microscopy measures the surface roughness and friction between the tip and the given sample. It is usually used for thin films. The atomic force microscope is a characterization technique for surfaces analysis. The surface of the given sample is scanned by a probe. Atomic Force Microscopy works on the principle of sensing forces between the atoms in the tip and in the sample [8]. There are many important parts, one of them is thin cantilever. It has sharp probe tip and its radius ranging from 10 nm to 50 nm. An optical system is used to measure deflection of that cantilever and for three dimensional piezo-electric scanners. The probe is a flexible cantilever—think of a diminutive diving board—with a tip attached to its underside. Combination of the surface forces (attractive and repulsive) affects the tip when tip is brought into the contact with the surface or in its proximity, or is tapping the surface. Bending and torsion occurs in cantilever because of those forces and is continuously measured via the deflection of reflected laser beam. In order to scan the predetermined area of the sample surface, the scanner moves that sample or, in 3D. Force may be monitored in between the tip scans the sample. The force is kept constant by moving the Cantilever. The ups and down motion of this cantilever represents the hills like and valleys like structure on the surface and is measured by reflected laser beam. This image can be translated by computer.

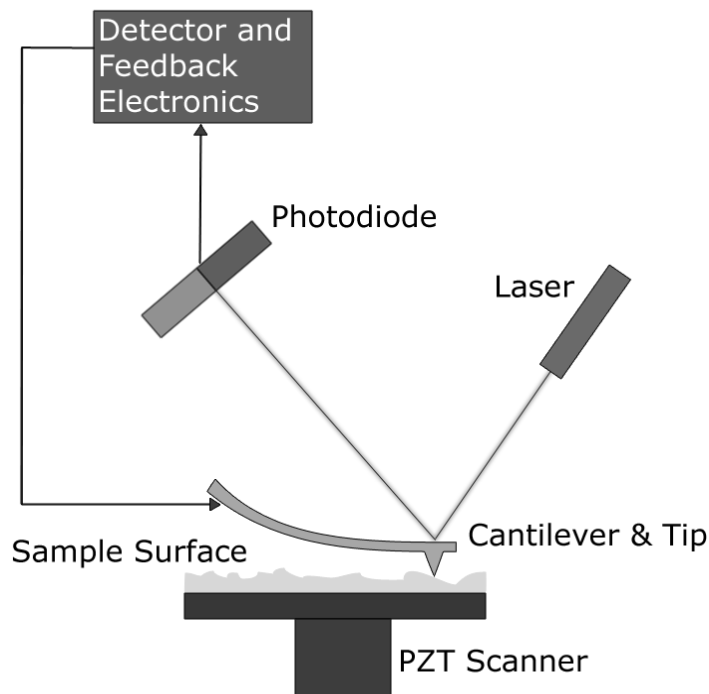


Figure 3. 4: Block diagram of AFM operation.

The van der Waal forces are commonly associated with Atomic Force Microscopy.

3.3 Optical characterization

3.3.1 Spectrophotometer

Optical properties of thin film include transmission, absorption, refractive index, band gap, absorption coefficient, and reflectance can be finding out by Spectrophotometer. The absorption gives very interesting optical properties which are very important for electronics devices. In semiconductors, there is very narrow conduction band and having wide valance band present, the absorption having energy equal to $h\nu = E_g$. At this stage, the electrons are transferred between valance and conduction bands without changing the voltage, this E_g is called the direct energy gaps. Group II-VI semiconductor materials having band related to this type.

Transmission or transmittance can be directly obtained from the film. The other properties may be calculated from the given transmission spectra. Transmission spectra of the samples were

recorded on UV-VIS/NIR spectrophotometer (Perkin Elmer Lambda 900), interfaced with a computer by UV-Win Laboratory software. Transmission is plotted versus wavelength as shown in the figure 4.3. Refractive index and thickness of films are measured with the help following formulas:

The refractive index (n) is measure by following formula.

$$n = \frac{[N + (N^2 - 4s^2)^{\frac{1}{2}}]}{2} \dots\dots\dots(3)$$

Where,

$$N = 1 + s^2 + 4s \left(\frac{T_{\max} - T_{\min}}{T_{\max} * T_{\min}} \right) \dots\dots\dots(4)$$

In above equations, s is the refractive index of glass (s = 1.52), T_{max} is the maximum transmission and T_{min} is very next minimum transmission as shown in the figure 5.

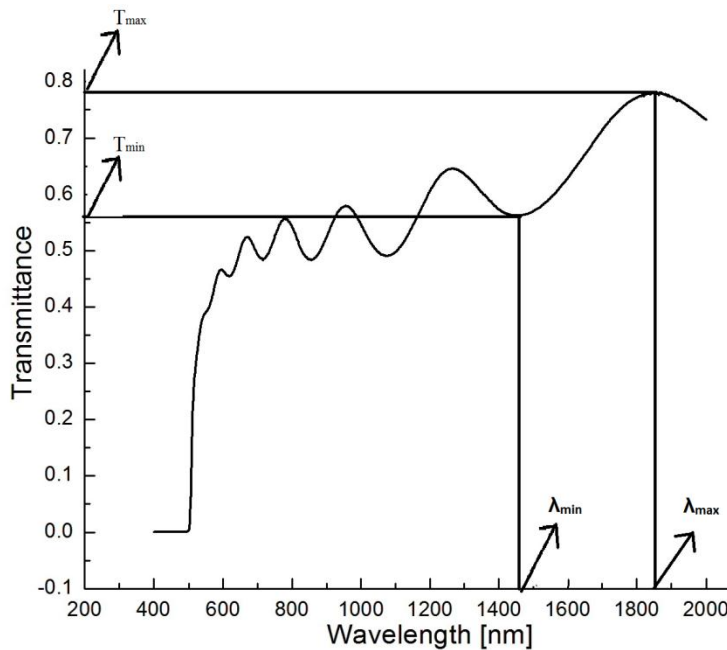


Figure 3. 5: Transmission spectrum to measure the thickness and refractive index

Thickness of the film is determined from the formula:

$$\frac{\lambda_{\max} \lambda_{\min}}{4n(\lambda_{\max} - \lambda_{\min})} \dots\dots\dots (5)$$

λ_{\max} , λ_{\min} are the values of wavelengths corresponding to maximum and minimum transmission respectively as shown in the figure.

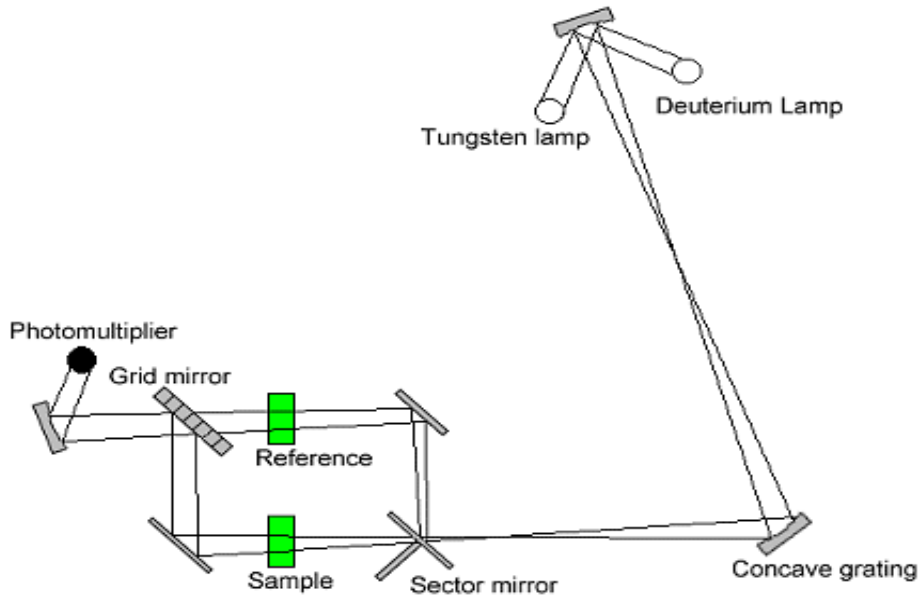


Figure 3. 6: Schematic of Spectrophotometer for transmittance [10].

3.4 Electrical Characterization

We can say that surface properties and effects in semiconductors especially in thin films have great influence on electrical properties. In electrical characterization, we have different parameters to be focused on it but in general we do concern with resistivity, mobility, charge carriers and doping type etc. Different methods can be used to find out electrical parameters.

3.4.1 Two-probe method

Generally 2-probe electrical measurement method is used for measuring resistivity and I-V curves. In this method Ohm’s law is used for calculating resistance which is given as,

$$R=V/I \dots\dots\dots (6)$$

Source meter is used in 2-probe electrical characterization technique. In this method, a current is passed through unknown resistance. The potential difference develops across the resistance and is measured and resistance is calculated using Ohm's law.



Figure 3. 7: Keithley 4200-SCS for Electrical Characterization [11]

3.4.2 The Hall Effect

The Hall Effect was discovered in 1874, by E. H. Hall effect is supported by the necessitate to find out accurately carrier concentration, dc electrical resistivity, mobility, Hall coefficient and sheet magneto resistance in case of metals and semiconductors thin films. In this experiment, an electric current is passed through the semiconductor block while a magnetic field **B** is applied perpendicular to the current as shown in Figure 8. Because of this setup a field is generated called as Hall voltage which is recorded perpendicular to the direction of current flow.

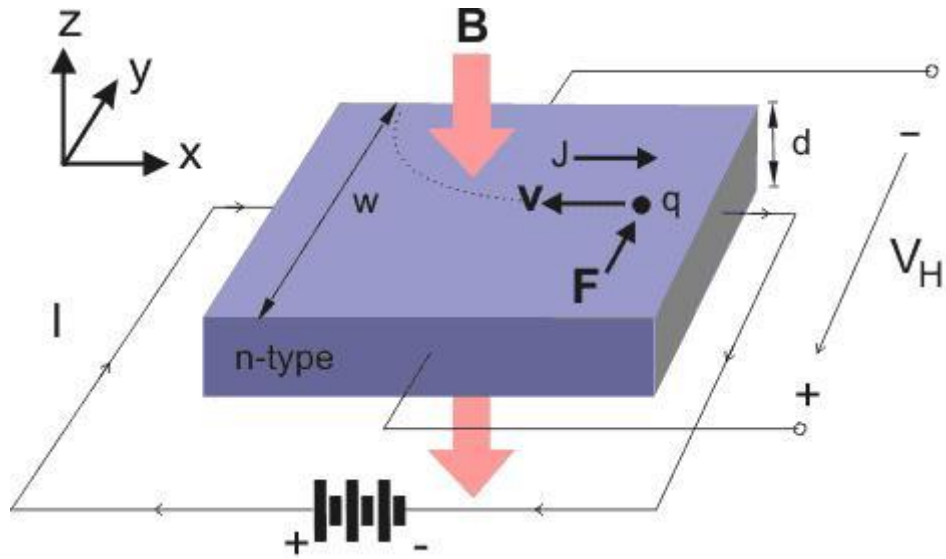
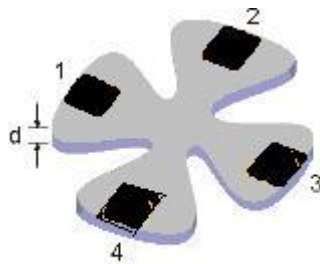


Figure 3. 8: Schematic diagram of the Hall Effect.

3.4.3 Van Der Pauw Method

To measure the resistivity of a thin, arbitrary-shaped sample with four Ohmic contacts Van der Pauw technique can be used. By using Van der Pauw method sheet resistance R_s of the sample is measured [13]. According to Van der Pauw demonstrated that there are two characteristics resistances, R_A and R_B , associated with the four terminals.



$$R_A = \frac{V_{43}}{I_{12}} , \quad R_B = \frac{V_{14}}{I_{23}}$$

Voltage measured across terminals 4 and 3 is V_{43} , and I_{12} is the current measure across terminals 1 and 2. Voltage measured across terminals 1 and 4 is V_{14} and I_{23} is the current measured across terminals 2 and 3. R_A and R_B relate to the sheet resistance through the Van-der Pauw equation.

$$\exp(-\pi \frac{R_A}{R_S}) + \exp(-\pi \frac{R_B}{R_S}) = 1 \dots\dots\dots (7)$$

This can be solved numerically for R_S . The resistivity can then be calculated using equation:

$$\rho = R_S t \dots\dots\dots (8)$$

By measuring Hall voltage V_H , in van der Pauw technique sheet carrier density n_s is determined. By keeping current and perpendicular magnetic field B constant, series of voltage is measured which corresponds to Hall voltage measurements. The sheet carrier density n_s can be calculated via

$$n_s = \frac{IB}{q|V_H|} \dots\dots\dots (9)$$

To avoid the errors, quality and size of ohmic contacts, accurate thickness and uniformity of sample is very important.

3.5 Characteristics Resistances via Van der Pauw technique:

3.5.1 Sheet Resistance

There are two characteristics resistances i.e. R_A and R_B which were established by Van der Pauw. Both resistances R_A and R_B are linked with the consequent terminals. As we have a van der pauw equation so both characteristics resistances i.e. R_A and R_B are correlated to the sheet resistance R_S via Van der Pauw equation. This Van der Pauw equation is stated below

$$\exp(-\rho R_A/R_S) + \exp(-\rho R_B/R_S) = 1 \dots\dots\dots (10)$$

Such numerical solution of Van der Pauw equation gives sheet resistance R_S . If one measures the sheet resistance with the help of Van der Pauw equation then one can easily estimate the bulk resistivity of thin-plate sample as well as the thickness of thin-plate sample following equation

$$\rho = R_S d \dots\dots\dots (11)$$

3.5.2 Sheet Density

With the help of known values of current, magnetic field and elementary charge, one can easily find out the sheet density n_s of charge carriers.

If Hall voltage is known then the sheet carrier density n_s can be easily calculated with equation after knowing the other parameters of equation

$$n_s = IB/q|V_H| \dots\dots\dots (12)$$

- The transverse voltage measured in a Hall probe has its origin in the magnetic force on a moving charge carrier. The magnetic force is $F_m = ev_d B$ where v_d the drift velocity of the charge. The current expressed in terms of the drift velocity is $I = neAv_d$. Where n is the density of charge carriers. Then $F = eIB/neA$.

At equilibrium

$$F_m = F_e = \frac{V_H e}{w} \dots\dots\dots (13)$$

And substituting gives

$$V_H = \frac{IB}{ned} \dots\dots\dots (14)$$

- Hall voltage also gives information about N-type and P-type semiconductors. If Hall voltage is positive, material is P-type and if Hall voltage is negative, material will be N-type.
- In a regular three-dimensional conductor, the **sheet resistance** can be find by this darivation

$$R = \rho \frac{L}{A} = \rho \frac{L}{Wt} \dots\dots\dots (15)$$

Where ρ represent resistivity, A denotes cross-sectional area and L represents length. We can write the area in term of multiple of length and thickness

By combining resistivity and thickness, the resistance may be represented as,

$$R = \frac{\rho L}{t W} = R_s \frac{L}{W} \dots\dots\dots (16)$$

Where R_s represents the sheet resistance.

3.5.3 Hall mobility

is the measure of the mobility of the electrons or holes in a semiconductor [13]. It can be easily calculated from the equation which state as

$$\mu = |V_H|/R_S IB = 1/(qn_s R_S) \dots\dots\dots (17)$$

Where V_H is hall voltage and R_S is sheet resistance

- **Bulk density, Bulk resistivity and Bulk conductivity** can be calculated.
- **Magneto resistance** deals with the change of resistivity of material when it is subjected to magnetic field. magneto resistance effects depends upon how much the change in the resistivity occurs when materials are subjected to magnetic field.

References

[1] K. L. Chopra and S. R. Das, Thin Film Solar Cells, Plenum Press, New York (1983).

[2] D. K. Schroder, Semiconductor materials and Device Characterization (2nd Edition), A Wiley-Interscience publication, John Wiley & Sons, Inc., (1998).

[3] K. L. Chopra and S. R. Das, Thin Film Solar Cells, Plenum Press, New York, (1983).

[4] D. K. Schroder, Semiconductor Materials and Device Characterization (2nd Ed.), John Wiley & Sons, Inc. (1998).

[5] B.D. Cullity, Element of X-Ray Diffraction, Addison-Wesley publishing Company, Inc. (1978)

[6] www.unl.edu/CMRAcfem/semoptic.htm.

- [7] B. E. Naltingk, Instrumentation Ref. Book 2nd Edition, Butterworth Heinemann Ltd. **92** (1995).
- [8] G. Binnig, C. F. Quate, C. Gerber, Phys. Rev. Lett. **56**, (1986) 930.
- [9] R. Howland and L. Benatar, A practical guide to Scanning Probe Microscopy, (2000).
- [10] <http://teaching.shu.ac.uk/hwb/chemistry/tutorials/molspec/uvvisab3.htm>
- [11] <http://nanohub.org/resources/10386>
- [12] <http://www.answers.com/topic/hall-mobility#ixzz1kyRC1aQ4>
- [13] V. Pauw, et al, Philips Research Reports**13**(1958) 1.

Chapter 4

Morphological and Structural Characterization of Ag and Cu Doped ZnTe

4.1 Fabrication of ZnTe Thin Film

ZnTe thin film was fabricated at Thermal Transport Laboratory by Close Space Sublimation (CSS) technique. Glass substrate was used to deposit ZnTe thin films. Before fabrication, glass substrate was ultrasonically cleaned with IPA. ZnTe powder was used to sublime from a graphite boat. Mica sheet was used as a substrate holder and also for thermal insulator between source and substrate. The source and substrate were separated by a distance of very less distance to get required deposition rate and better uniform films. During this experimentation, the source and substrate were kept at 500⁰C and 450⁰C respectively. The pressure of the evaporation chamber was $\approx 10^{-2}$ mbar.

Thin films of different thickness were obtained because there was no thickness monitor installed in this apparatus to control the thickness. Films had good adhesion with the glass substrate, as tested by squash tape test. These films were thermally annealed at 300 ⁰C in a vacuum chamber for 1hour. ZnTe thin films fabricated by CSS method were doped with Ag and Cu using same technique to decrease their resistivity. Doping time was changed under same temperature and vacuum conditions. After doping, these films were annealed at 380⁰C for 1hour.

4.2 Structural Analysis

The X-ray diffraction pattern (XRD) of a typical ZnTe film in the as-deposited, annealed and doped condition is shown in the Fig.4.1.

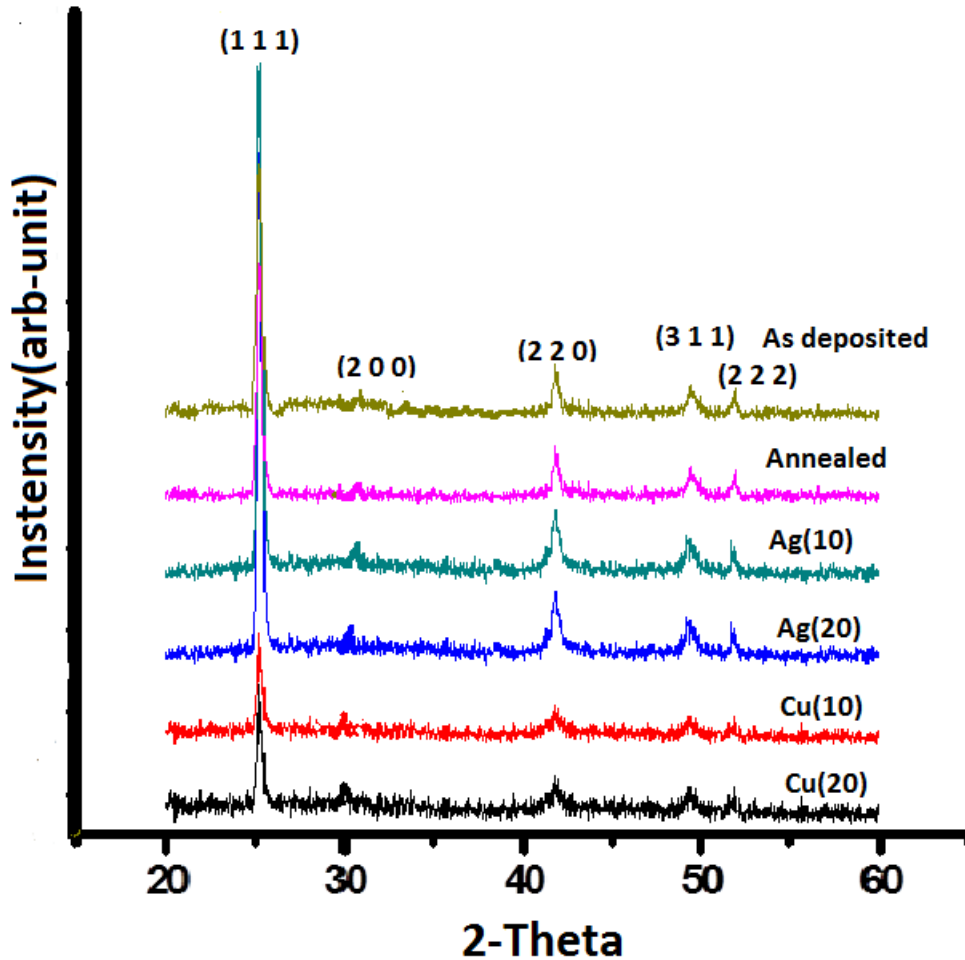


Figure 4.1: XRD pattern for ZnTe sample

It is detected from the figure that, the XRD of undoped ZnTe film is found to be polycrystalline with preferential orientation along the (111) plane, the other secondary peaks visible are (200), (220), (311) and (331). All the peaks are accompanied with cubic ZnTe and no major Zn or Te peaks are found. That confirms the doping of silver and copper As is evident from the figure, all the fabricated ZnTe thin films with varying conditions and dopant concentrations exhibit single phase zinc blende cubic structure having no extra detectible impurities. All the peaks in the patterns match well with the characteristic reflections of Zn and Te found in good agreement with the previous work [1].

XRD pattern of Cu doped and Ag doped ZnTe thin film is also shown in the Fig.4.1. Again the XRD pattern shows a cubic structure with preferred orientation along [111] direction. No major difference was observed between as deposited and doped XRD patterns. The sharpness of the peak increases for Cu doped ZnTe thin films which in turn decreases the FWHM, while the

sharpness of the peak decreases for Ag doped ZnTe thin films which in turn increases the FWHM [2]. The broad peaks signify lower crystallite size of the fabricated thin films. The average crystallite size for each composition was calculated using the standard Scherer's formula from the line broadening of the XRD peak corresponding to the total average peaks of the planes of the zinc blende cubic structure.

$$L = \frac{K\lambda}{B\cos\theta}$$

Where K (K=0.94) is the Scherer's constant, L is the crystallite size, λ (CuK $_{\alpha}$ = 1.5404Å) is the wavelength of the X-ray and B is the FWHM of diffraction peak at θ .

Table 4.1: Crystallite size of ZnTe and doped ZnTe thin films.

Sample Name			Crystallite Size (nm)
ZnTe (Annealed)			17.64
Dopant	Time (minutes)	Concentration (%)	
Cu	10	0.45	25.24
Cu	20	0.45	25.7
Ag	10	1.60	21.0
Ag	20	1.60	21.26

The average crystallite size (t) and lattice parameter (a) are found within range 17-30nm and 6.05Å as shown in the Table 4.1. The increase in crystallite for dopants actually increases the crystallinity of thin films. Due to small concentrations of Cu and Ag incorporated in ZnTe thin films, the Cu and Ag peaks are not seen in the XRD pattern.

4.3 Surface Morphology

Morphology of the synthesized film was characterized by Scanning Electron Microscope (SEM) of as deposited ZnTe thin film fabricated by close space sublimation (CSS) technique under vacuum of 10⁻²mbar. It should be noted that the ZnTe thin film shows high resistivity and this resistivity causes the charge accumulation at the surface of ZnTe and this will cause the reflection of incident beam like a mirror. So, to avoid this problem the ZnTe thin films were coated with gold film with thickness 200Å⁰ and further the conductivity is improved. The

micrographs were obtained at different scanning resolutions shown in Fig 4.2 and 4.3. The fig 4.2 shows scanning micrograph at lower resolution confirm that the thin film in the form of particles in nanometer size is deposited uniformly with very small amount of porosity. Further morphological analyses were done at high resolution at 30,000X shown in fig 4.3 to confirm the particle size and distribution. It is observed from fig 4.3 that the particle size was found in range 48-241 nm.

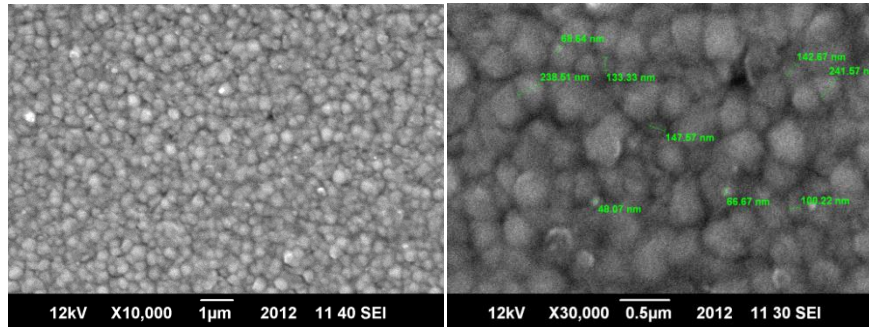


Figure 4.2: SEM image at lower Resolution

Figure 4.3: SEM image at high Resolution

For the thin film uniformity in particle/film distribution with very less porosity is desired for this ZnTe films were annealed at 300C0 for 1hours. The effect of temperature on microstructure can easily be seen from Figures 4.4 and 4.5. It is observed that the particle/film coarsening due diffusion of Zn and Te grains with temperature and this leads to decrease in porosity while the films become thicker.

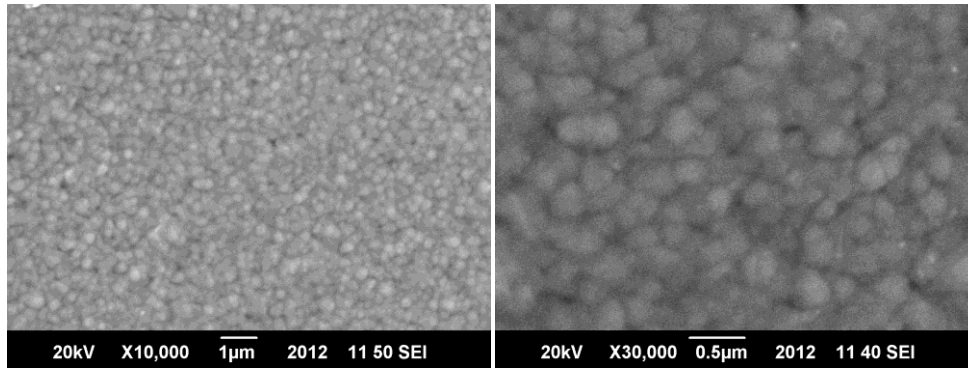


Figure 4.4: Effect of Temperature on Microstructure

Figure 4.5: Effect of temperature on Microstructure

The effect of dopants Cu and Ag with varying doping time (15 and 20 min) on morphology and microstructures are studied. Fig 4.6 and 4.7 represents the micrograph for Ag doped ZnTe sample. The dopant material influences various physical parameters e.g. porosity, density etc. The distribution of grains can be easily seen in micrograph and further surface roughness is enhanced with dopant concentration. The annealing enhances the diffusion in grains having different crystalline orientations which can also be confirmed by EDX. The morphology and microstructure Cu doped ZnTe film at different magnification and resolution are represented by Fig 4.8 and 4.9. It is clear through the micrographs the whole structure is divided into two types of different grains with almost uniform sizes differentiate the dopant material from the ZnTe structure.

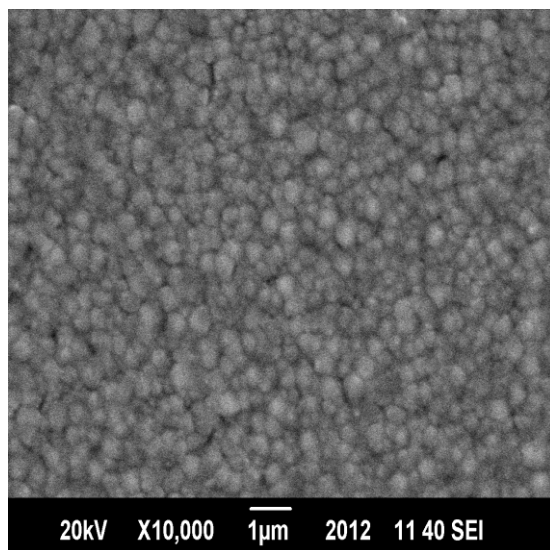


Figure 4.6: Microstructure of Ag Doped ZnTe at lower magnification

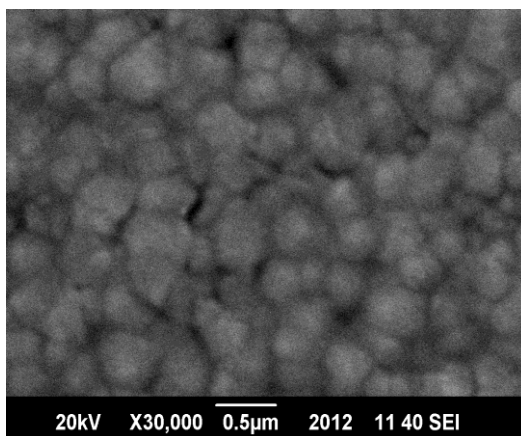


Figure 4.7: Microstructure of Ag Doped ZnTe at higher magnification

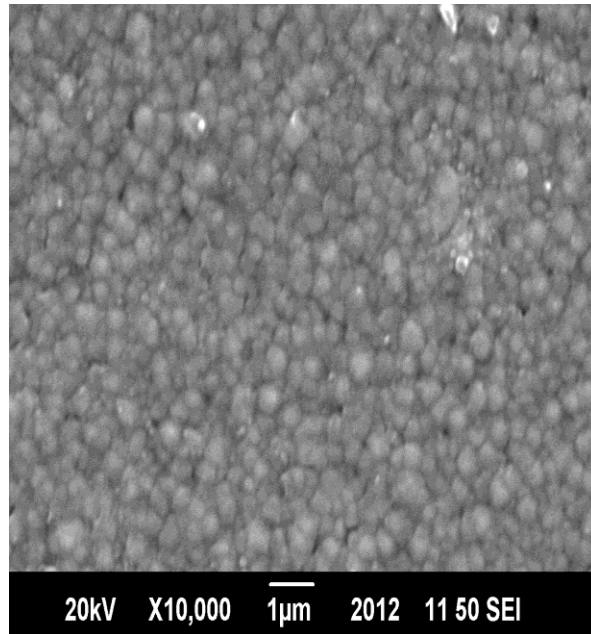


Figure 4.8: Micrographs of Cu Doped ZnTe at low resolution

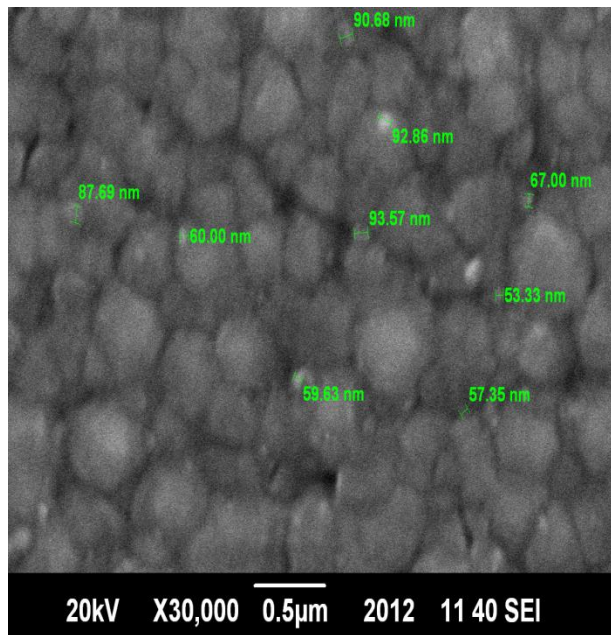


Figure 4.9: Micrographs of Cu Doped ZnTe at high resolution

4.4 Compositional Analysis

The compositional analysis of the fabricated film was performed using energy dispersive X-Ray spectroscopy (EDS). Table 4.2 represents the compositional analysis of ZnTe and Cu and Ag

doped ZnTe thin films. EDS analysis confirms large mass percentage of ZnTe as shown in the table 4.2. No extra elements were observed in the compositional analysis of as deposited ZnTe thin films. From the table it is also confirmed that 1.53 atomic % Ag doped ZnTe was observed with concentration of 1.60%. Similarly 0.72 atomic % Cu doped ZnTe was observed with concentration of 0.45%.

Table 4.2: EDS analysis

Element	KeV	Mass (%)	Atomic (%)
Zn	1.012	25.41	39.94
Te	3.768	74.59	60.06
Ag Doped			
Zn	1.012	24.52	38.71
Ag (10)	2.983	1.60	1.53
Ag (20)	2.983	2.46	2.37
Te	3.768	73.89	59.76
Cu Doped			
Cu (10)	0.930	0.45	0.72
Cu (20)	0.930	0.60	0.97
Zn	1.012	26.02	40.56
Te	3.768	73.53	58.72

4.5 Morphological Study

4.5.1 As deposited ZnTe and Annealed ZnTe Thin Films

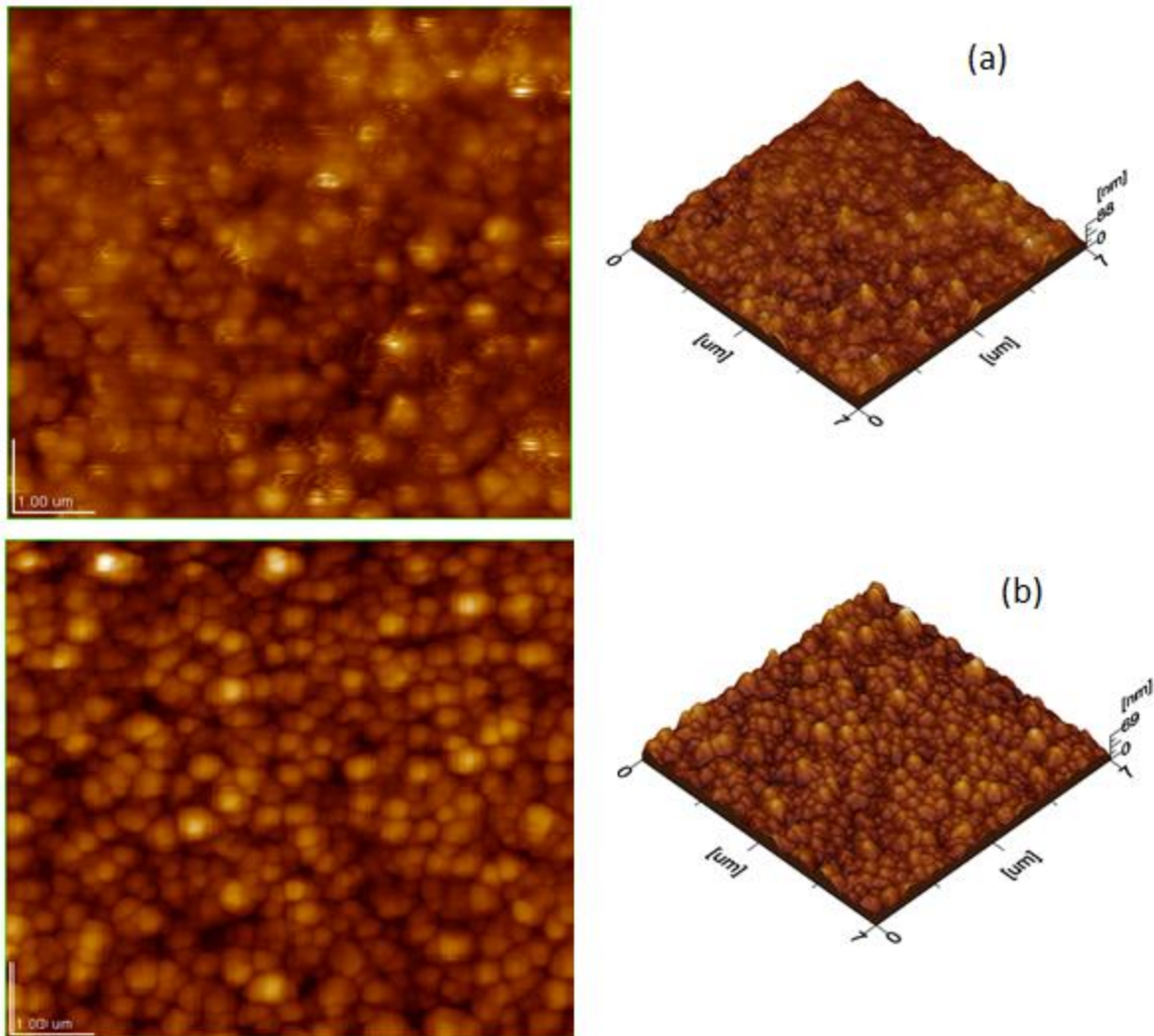


Figure 4.10: AFM images of ZnTe thin films (a) as deposited (b) annealed at 380⁰C for 1 hour.

Figure 4.13 shows AFM images of as deposited and annealed ZnTe thin films. It is clearly evident from the comparison of as deposited and annealed samples that smoothness, compactness and regularity in films have increased after annealing. While average roughness have decreased this is again in agreement with above statement. So it can be thought that with

the high temperature during the deposition process the crystals got oriented properly in lattice as depicted in XRD results.

4.5.2 Ag (20 min doped) Annealed at 380⁰C for 1hour

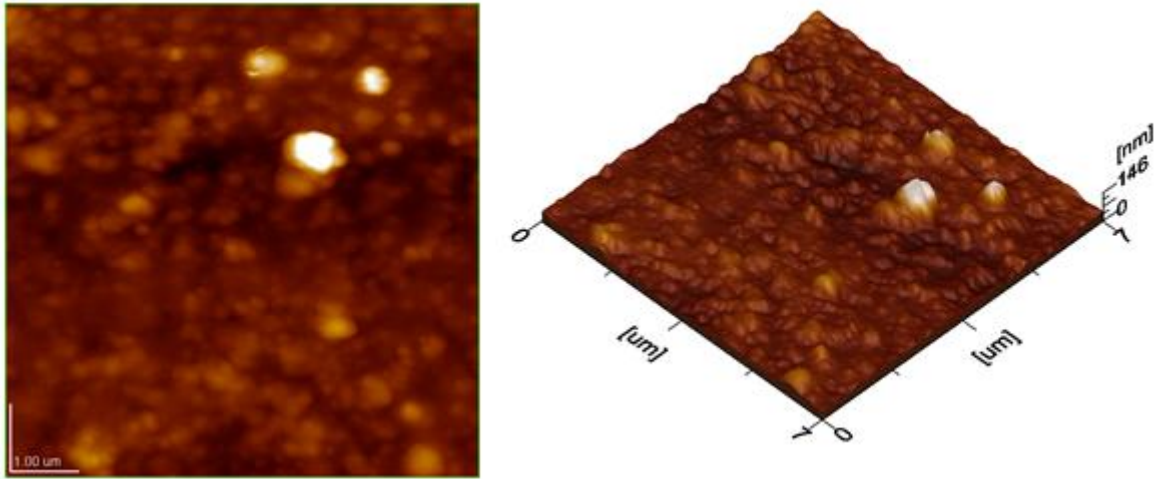


Figure 4.11: Morphology of Ag (20 min doped) annealed at 380⁰C for 1hour

Figure 4.14 shows AFM images of Ag doped ZnTe thin films. In Ag doped samples the roughness have increased and film is more irregular in z-axis. There are some comparatively large grains in film that may be due to presence of Ag inclusion at that spot which acted as preferred nucleation site.

4.5.3 Cu (10min doped) Annealed at 380⁰C

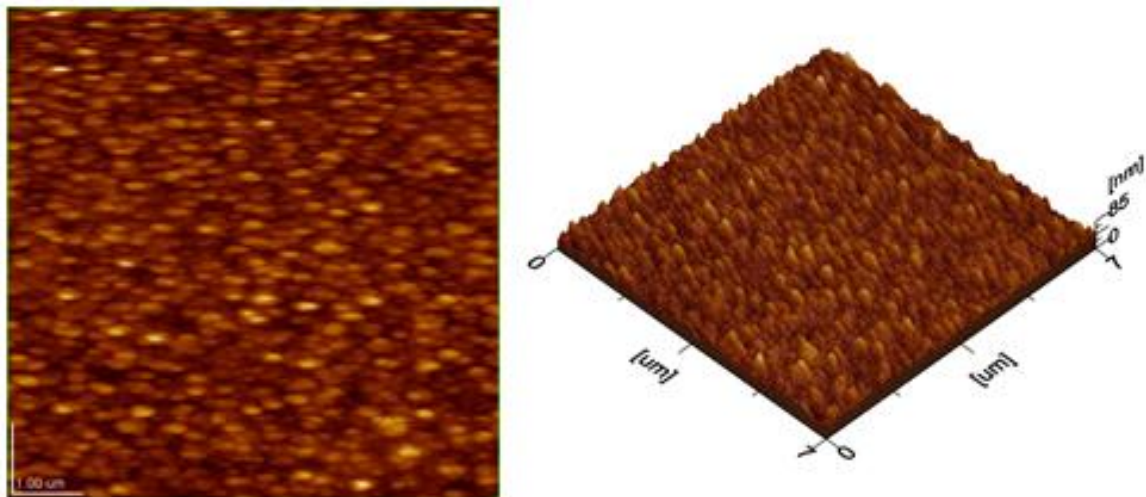


Figure 4.12: Morphology of Cu (10min doped) doped ZnTe and annealed at 380⁰C

Figure 4.15 shows AFM images of Cu doped ZnTe thin films. Copper doped samples have more smooth topography as compared with Ag doped and have lower value of average roughness. Grain sizes are ranging from 17 to 30 nm with a compact structure of film. So we can say that Copper gets easily doped and don't form its own inclusions and is distributed in the lattice of zinc Telluride.

References

- [1] Akram K.S.Aqili, et al, applied surface science, 167 2000. (1–11)
- [2] V.S. John et al, Solid-State Electronics 49 (2005) 3–7

Chapter 5

Electrical Characterization of As Deposited, Ag and Cu Doped ZnTe Thin films

5.1 General Electrical Properties of ZnTe Films

P-type films are those which contain more concentration of holes as compared to electrons, as charge carrier are holes in those films so those films are p-type films [1-3]. Un-doped fabricated ZnTe thin films are of p-type. The resistivities of such films are of range greater than 10^6 ohm-cm [4, 5]. Using non-stoichiometric ZnTe films, the resistivity can be reduced like as in case of thermal evaporation which should be at low temperature of substrate. Doping of Cu, N and Sb [5, 6-7] result in reduction of resistivity below 0.1 ohm-cm. ZnTe films doped Cu by method of vacuum evaporation result in reduction of resistivity from order of greater than 10^6 ohm-cm for un-doped ZnTe films to 5×10^{-3} ohm-cm for Cu doped ZnTe thin films, and in case of the carrier mobility, it ranges from $0.1 \text{ cm}^2\text{v}^{-1}\text{s}^{-1}$ to $1 \text{ cm}^2\text{v}^{-1}\text{s}^{-1}$. Using method of sputtering, Cu-doped films can also be obtained with characteristics of low resistivity. Temperature of substrate play a vital role in describing about resistivity values i.e. ~ 6 to ~ 0.03 ohm-cm [8, 9]. Using doping by MOVPE [6], the resistivity can be reduced to ~ 1 ohm-cm with the hall mobility of $8.5 \text{ cm}^2\text{v}^{-1}\text{s}^{-1}$ and with more carrier concentration of $\sim 10^{18} \text{ cm}^{-3}$. In case of Nitrogen doping [10] by using method of laser ablation result in enhancement of the carrier density to $\sim 2 \times 10^{18} \text{ cm}^{-3}$.

5.2 Hall Effect Measurement System (HMS-5000)

Electrical characterization of ZnTe thin films have been done with the help of Ecopia 5000 Hall Effect Measurement System. Thickness of these all ZnTe thin films for electrical characterization determined with help of Spectrophotometer. Thickness of thin film has been found out i.e. 2.56 micro-meters. Contacts have been made on four corners of thin films. These thin films shaped with square geometry [11]. Material of Indium tin has used for making contacts

on four corners of square ZnTe thin films for Hall Effect measurements. These all electrical measurement has been done at temperature i.e. 300K.

5.2.1 Hall coefficient of ZnTe thin films

Hall coefficients for ‘as deposited ZnTe thin film’ was found with the help of Ecopia 5000 Hall Effect Measurements System and hall coefficient is found to be positive which indicate that ZnTe thin film is of p-type [2,3] which shows this ‘as deposited film’ is with more concentration of holes rather than electrons as charge carriers. Nature of such p-type film can be changed with help of doping of Cu and Ag. Our observations agree with the earlier reported data [1]. Different features of charge carriers for Cu-doped ZnTe and for Ag-doped ZnTe have been observed. The nature of carrier which found in case of as deposited ZnTe, Cu-doped ZnTe and Ag-doped ZnTe thin films is shown in table as below. Polarity of hall coefficient describe type of material either it is n-type or p-type. If material has positive hall coefficient then it is p-type and if it has negative hall coefficient then it termed as n-type material.

Table 5. 1: Nature of Material and type of charge carrier

Sample Name	Hall Coefficients	Nature of Material
a=As Deposited	Positive	p-Type
b=10 min Cu Doped	Negative	n-Type
c=20 min Cu Doped	Negative	n-Type
d=10 min Ag Doped	Positive	p-type
e=20 min Ag Doped	Negative	n-type

p-type materials are with more concentration of holes as charge carriers and n-type materials are with more concentration of electrons as charge carrier.

5.2.2 Mobility and concentration for ZnTe thin films

With the help of Ecopia 5000 Hall measurements system, mobility and concentrations have been measured for as deposited ZnTe thin films and for Cu doped and Ag doped ZnTe films using indium tin contacts. Table shows that bulk concentration (cm^{-3}), sheet concentration (cm^{-2}) and mobility (cm^2/Vs) for these thin films. Sheet concentration according to surface density of films and bulk concentrations according to bulk density of thin films have been discussed here. Bulk Concentration variations for as deposited ZnTe and Cu doped ZnTe samples are shown in figures 5.1 and 5.2.

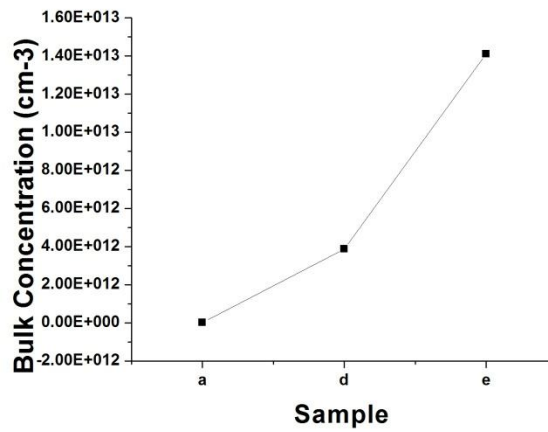


Figure 5. 1: Bulk Concentration for as deposited ZnTe and Ag Doped ZnTe samples

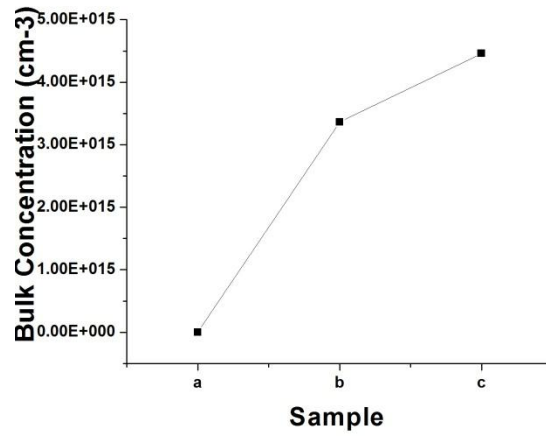


Figure 5. 2: Bulk Concentration for as deposited ZnTe and Cu doped ZnTe samples

Sheet concentrations for as deposited and doped samples of ZnTe are shown as in figures 5.3 and 5.4.

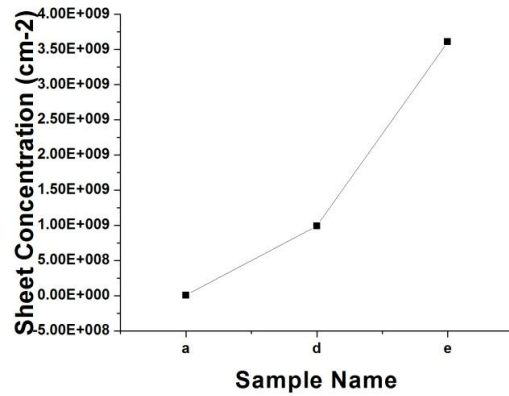


Figure 5. 3: Sheet Concentration for as deposited ZnTe and Ag doped ZnTe samples

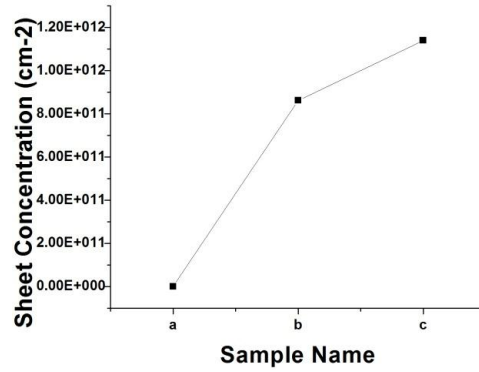


Figure 5. 4: Sheet Concentration for as deposited ZnTe and Cu doped ZnTe samples
 Motilities for as deposited ZnTe and Ag or Cu doped samples are as follow in figures 5.5 and 5.6.

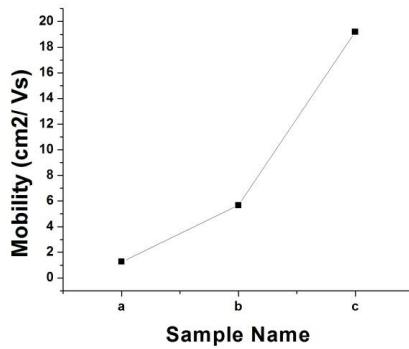


Figure 5. 5: Mobility variations for as deposited ZnTe and Cu doped ZnTe

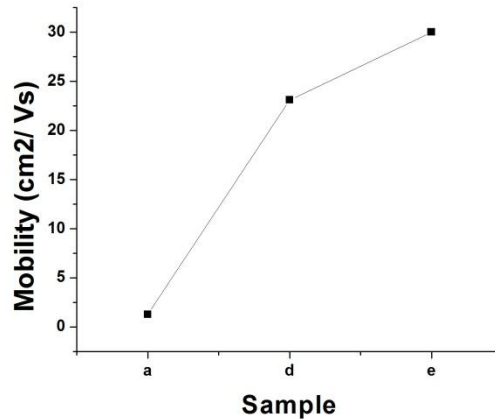


Figure 5. 6: Mobility variations for as deposited ZnTe and Ag doped ZnTe samples

Table for sheet concentration, bulk concentrations and motilities for as deposited ZnTe and Ag doped ZnTe and Cu doped ZnTe samples are as shown in table.

Table 5. 2: Sheet concentration, bulk concentration and mobility for as deposited and doped ZnTe films

Sample Name	Sheet Concentration(cm^{-2})	Bulk Concentration(cm^{-3})	Mobility (cm^2/V_s)
a=As Deposited ZnTe	-4.42E+06	-1.70E+10	1.26
b=10 min Cu Doped ZnTe	8.62E+11	3.36E+15	5.67
c=20 min Cu Doped ZnTe	-1.14E+12	-4.46E+15	1.92E+01
d=10 min Ag Doped ZnTe	9.91E+08	3.87E+12	2.31E+01
e=20 min Ag Doped ZnTe	3.61E+09	1.41E+13	3.00E+01

Mobility for these as deposited ZnTe and Cu/Ag doped ZnTe thin films are ranges from 1.26 to 3.00E+01 cm^2/V_s and similarly bulk concentrations for same thin films are ranges from 10E+10 to 10E+15 cm^{-3} which is in agreement with previous reported data as well [3]. Similarly sheet concentrations ranges from 10E+6 to 10E+12 cm^{-2} . As mobility and conductivity has direct relations and conductivity has inverse relation with the resistivity so with increase of carrier mobility, resistivity decrease or conductivity increased. With increase of concentration of Cu, mobility of carriers has become improved in this case. Similarly with increase of concentration of Ag, mobility again became better. So as a result, with increasing concentration of conductive dopant, mobility of carriers has also improved.

5.2.3 Resistivity measurements using van der pauw technique for ZnTe films

Using Ecopia 5000 system, resistivity measurements of as deposited ZnTe and for Ag/Cu doped ZnTe thin films have been done. Van der Pauw technique is four probe techniques for resistivity calculations. With help of Van der Pauw technique, resistivity is measured. At room

temperature for ZnTe thin films, resistivity is found to be the order of greater than 10^6 Ohm-cm, which has good agreement with the previous reported data [1-5]. Resistivity variations for as deposited and Ag/Cu Doped samples are shown in figures 5.7 and 5.8.

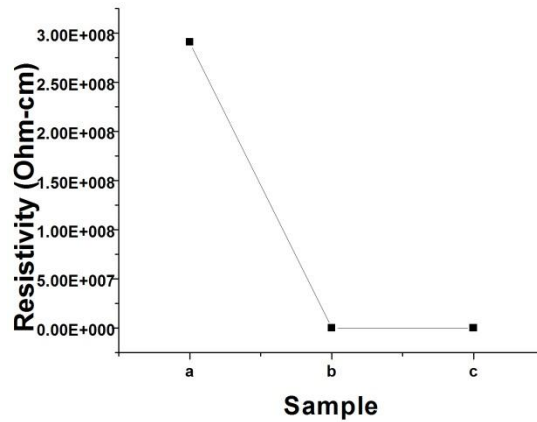


Figure 5. 7: Change in resistivity for as deposited ZnTe and Cu doped ZnTe

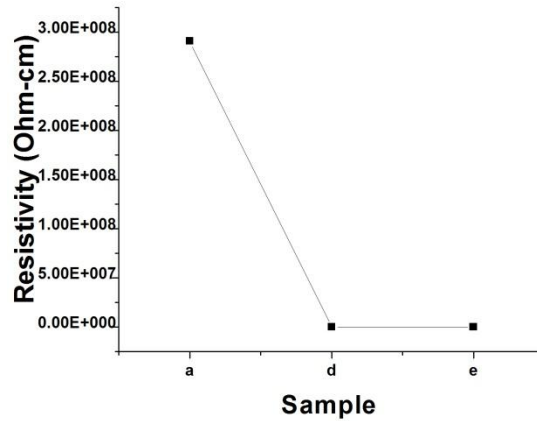


Figure 5. 8: Change in resistivity for as deposited ZnTe and Ag doped ZnTe

The resistivity values for as deposited ZnTe and Ag/Cu doped ZnTe are shown in table 5.3.

Table 5. 3: Resistivity for ZnTe films

Sample Name	Resistivity (Ohm-cm)
As Deposited ZnTe	2.91E+08
10 min Cu Doped ZnTe	1.49E+03
20 min Cu Doped ZnTe	6.43E+01
10 min Ag Doped ZnTe	3.96E+04
20 min Ag Doped ZnTe	6.02E+04

5.2.4 Conductivity for ZnTe thin films

As resistivity has direct relation with sheet resistance (R_s) using

$$\text{Resistivity} = \text{sheet resistance} \times \text{thickness}$$

Knowing about the thickness's of these films are used to calculate sheet resistance of these thin films if one has knowledge about dc electrical resistivity.

The below table shows that with doping of Ag or Cu result in reduction of resistivity. As Resistivity has inverse relation with conductivity so by more concentration of Ag/Cu [6], conductivity increased. Conductivity values how increase with doping of Ag/Cu are shown in figures 5.9 and 5.10.

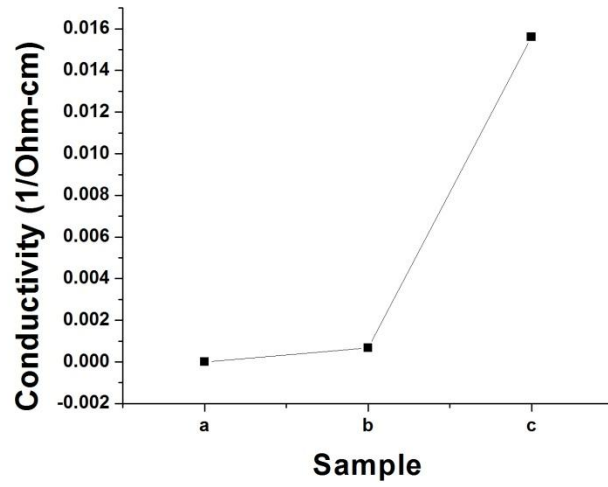


Figure 5. 9: Conductivity comparison for as deposited ZnTe and Cu doped ZnTe samples

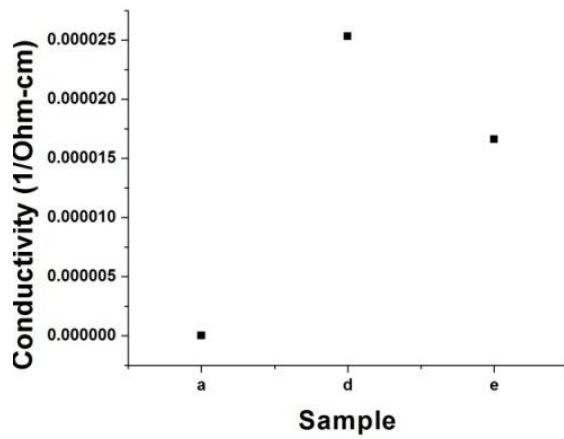


Figure 5. 10: Conductivity comparison for as deposited ZnTe and Ag doped ZnTe samples

Table shows how the conductivity increases with doping of Ag or Cu.

Table 5. 4: Conductivity for ZnTe films

Sample Name	Conductivity (1/Ohm-cm)
a=As Deposited ZnTe	3.44E-09
b=10 min Cu Doped ZnTe	6.73E-04
c=20 min Cu Doped ZnTe	1.56E-02
d=10 min Ag Doped ZnTe	2.53E-05
e=20 min Ag Doped ZnTe	1.66E-05

5.2.5 Sheet magneto-resistance for ZnTe thin films

Using Ecopia 5000 system, magneto resistance has been determined for ZnTe thin samples i.e. as deposited samples, Cu-doped ZnTe samples and Ag-doped ZnTe samples. Contacts of Indium tin was made on ZnTe thin films for four probe electrical characterization [11]. Samples of ZnTe thin films were with square geometry. Effect of sheet magneto resistance appeared when ZnTe thin films were subjected to a magnetic field which resulted in a change of resistivity of ZnTe thin films. Sheet magneto-resistance effect depends upon relative direction of applied magnetic field with respect to current and applied magnetic field itself. With subject of constant magnetic field of strength 0.55T, sheet magneto resistance for ZnTe thin films with different concentrations of Ag/Cu has been shown in table as well in figure 5.11.

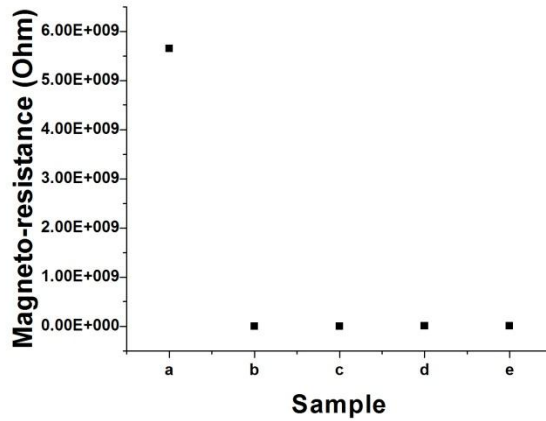


Figure 5. 11: Magneto-resistance variations for as deposited and Ag/Cu doped samples

Table 5. 5: Magneto-resistance for as deposited and doped ZnTe samples

Sample Name	Sheet Magneto-resistance (Ohm)
As Deposited ZnTe	5.65E+09
10 min Cu Doped ZnTe	2.59E+04
20 min Cu Doped ZnTe	1.72E+04
10 min Ag Doped ZnTe	1.38E+06
20 min Ag Doped ZnTe	2.40E+06

As a result, one can conclude that ‘As deposited sample’ of ZnTe has high sheet magneto-resistance i.e. order of 10 power 9 but when as deposited sample was doped with 10 mint copper concentration and then it was subjected with constant magnetic field of 0.55 Tesla [11] then sheet magneto-resistance has reduced to order of power 4, and when time for concentration was

increased to 20 mint and then there occur more reduction in sheet magneto-resistance. Similar case was observed in case of doping of silver into ZnTe thin films.

References

- [1] H.M. Brown, D.E. Brodie, Can, J. Phys., 50 (1972) 2512.
- [2] J.B. Webb, D.E. Brodie, Can, J. Phys., 52 (1974) 2240.
- [3] J.B. Webb, D.E. Brodie, Can, J. Phys., 53 (1975) 1415.
- [4] S.Kobayashi, N.Salto, T.Shibuya, Jpn. J. Appl. Phys., 19 (1980) 1199.
- [5] C.J.Moore, B.S. Bharaj, D.E. Brodie, Can. J.Phys., 59 (1981) 924.
- [6] W.Kuhn, H.P.Wagnert, H. Stanzi, K.Wolf, S.Lankes, Semicond, Sci, Technol., 6 (1991) AI05.
- [7] M.Nishio, K.Hayashide, Q, Guo, H.Ogawa, Applied Surface Science, 169-170 (201) 227.
- [8] T.A.Gessert, T.J.Coutts, 12th NREL Photovoltaic Program Review, (1993) 345.
- [9] T.A.Gessert, A.R.Mason, R.C.Reedy, R.Matson, T.J.Coutts, J. Electronic Materials , 24 (1995) 1443.
- [10] M.Nishio, Q.Guo, H.Ogawa, Thin Solid Films, 343-344 (1999) 512.
- [11] www.ecopia.com/HMS-5000 Manual.

Chapter6

Optical Characterization

To study the optical properties of thin films are very significant for various application point of view including interference devices, as well as optoelectronics, solar cells, integrated optics, optical sensor technology and micro-electronics. Regarding characterization tools different methods are being used such as spectrophotometric, interferometric, ellipometric, photothermal and combined methods as well.

Transmission of films is the only property, which is obtained directly from the film [1]. The rest are inferred from the transmission plots .transmission can be recorded by using an instrument known as spectrophotometer

6.1 Optical Analysis

The study of optical properties, as transmission, refractive index and energy gap are of great importance regarding any material used in opto-electronic applications. The UV-VIS /NIR spectrophotometer (Perkin Elmer Lambda 950) and UV-WinLab software were used to measure the transmission spectra of all samples (before and after doping) ,all parameters were calculated from transmission spectra.

6.1.1 Calculation of Band Gap, Refractive Index and Thickness

From Swanepoel model the refractive index and thickness of thin films can be calculated [2]. The refractive index can be calculated as

$$n = [N + (N^2 - 4s^2)^{1/2}] / 2 \dots\dots\dots 1$$

Where s is refractive index of the substrate, N is number of oscillations

$$N = 1 + s^2 + 4s(T_M - T_m) / T_M T_m \dots\dots\dots 2$$

Where T_M and T_m are the Transmission maxima and minima respectively.

Thickness of the films can be calculated with the help of formula

$$d = (1/4n) \times (\lambda_m \lambda_M / (\lambda_m - \lambda_M)) \dots\dots\dots 3$$

Where d is the thickness. λ_m is the minima and λ_M is the maximum value of wavelength taken from the transmission curve

As optical band gap decreases from 2.2384 eV to 2.2122 eV also XRD structure changes, intensity varies from 1500CPS to 100 CPS.

ZnTe fabricated under vacuum in Close Spaced Sublimation Technique (CSS) in structural properties preferred orientation is (111) and polycrystalline in nature, by annealing these planes increases their intensity and doping of these films shows that there is silver clearly show in these peaks and intensity level also changes.

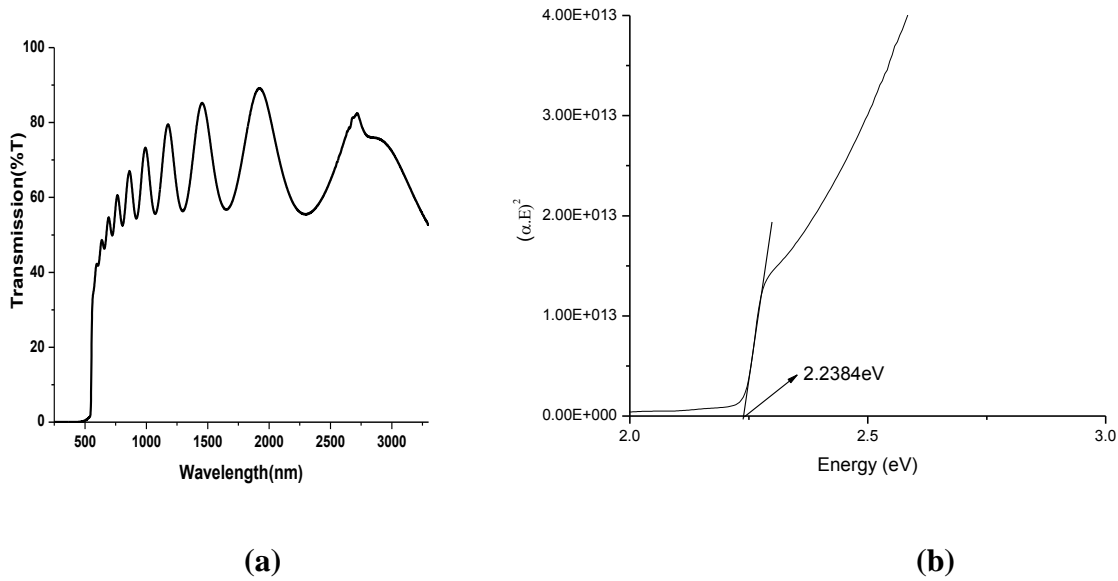


Figure 6. 1:(a-b): Transmission vs.Wavelength

Figure 6.1 (a) shows the relation between wavelength and transmission of as deposited ZnTe film and figure (b) shows the optical band gap of as deposited

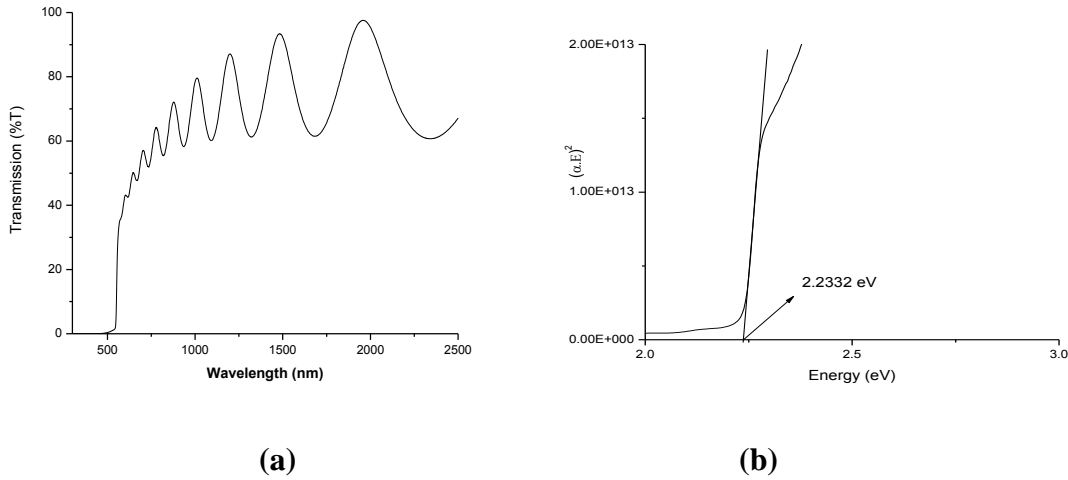


Figure 6. 2: (a-b) Annealed before doping at 300⁰C for 1hour

Fig. 6.2 shows optical characterization of annealed samples. As Deposited Maximum Transmission is **89** % but after annealing at 300C for 1 hour it is increased by **93** % also optical band gap of as deposited is 2.2384 eV and annealed at 300 C for 1 hour is 2.2332 eV.

6.2 Comparison of As deposited and Annealed ZnTe

The transmission spectrum of as-deposited sample and annealed sample are shown in Fig.

6.3

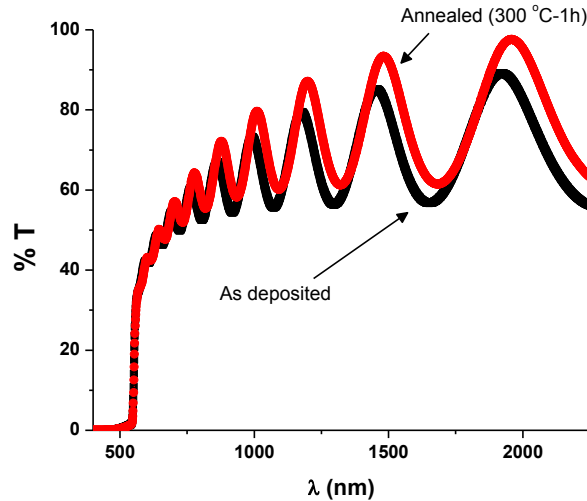


Figure 6. 3: Transmission spectrum of as deposited sample and annealed sample

Sudden fall in the transmission region above the wavelength (500nm) shows that, band gap of ZnTe occurs in this region. The ultraviolet rays and x-rays are absorbed, as these has more energy than the energy band gap of ZnTe. On the other hand entire infrared region is transmitted. Figure 6.3 in red color shows that transmittance behavior of as deposited and heating at 300°C for one hour. The obtained response confirms the improvement of transmittance and crystallinity of the films.

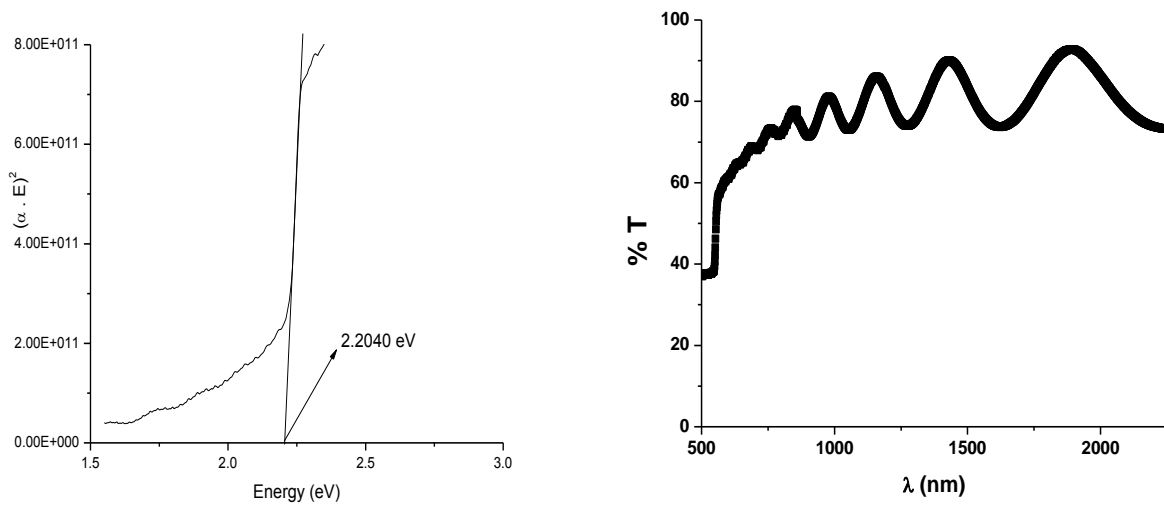


Figure 6.4: (a) $E_g = 2.2040\text{eV}$

(b) ZnTe Cu doping (5min) annealed after doping

Figure 6.4 (a) shows the band gap of ZnTe sample after doping Cu for 5min. Band gap of the samples comes out to be 2.2040 eV as shown in figure 6.4 (a) while figure 6.4 (b) shows the optical spectra of sample.

6.3 Copper Doping Effect

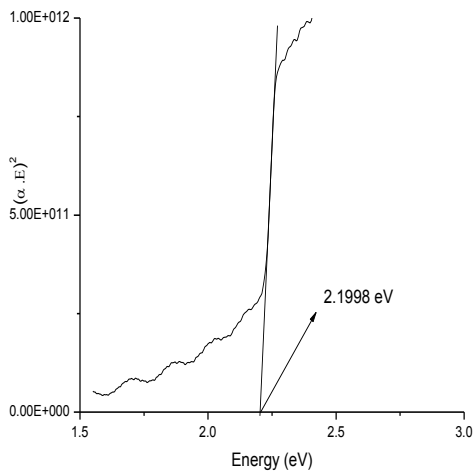
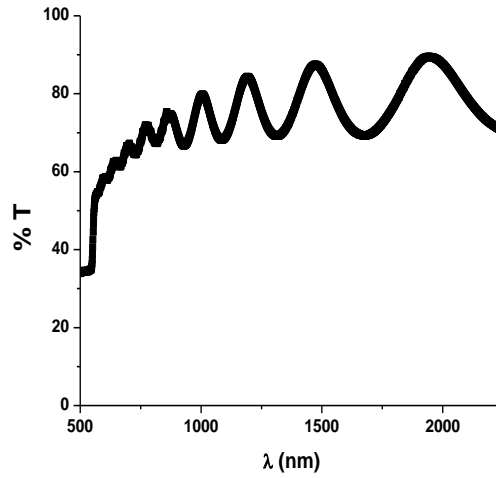


Figure 6. 5: (a) $E_g = 2.1998\text{eV}$



(b) ZnTeCu doping (sample) annealed after doping

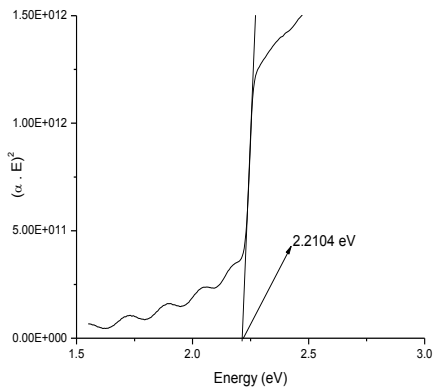
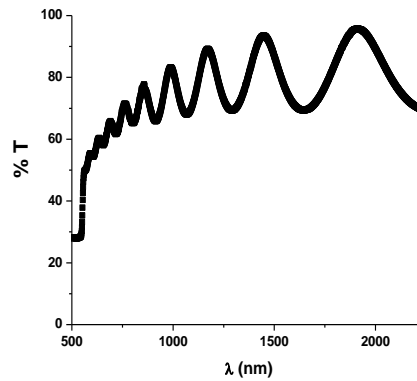


Figure 6. 6: (a) $E_g = 2.2104\text{eV}$



(b) ZnTe Doping (15 mint)annealed after doping

Fig. 6.6 (a) shows the band gap of Cu being doped in ZnTe samples for 15 min. Band gap increases from that of 5 min sample while (b) part shows the transmission behavior of 10 min doped sample.,

6.4 Silver Doping Effect

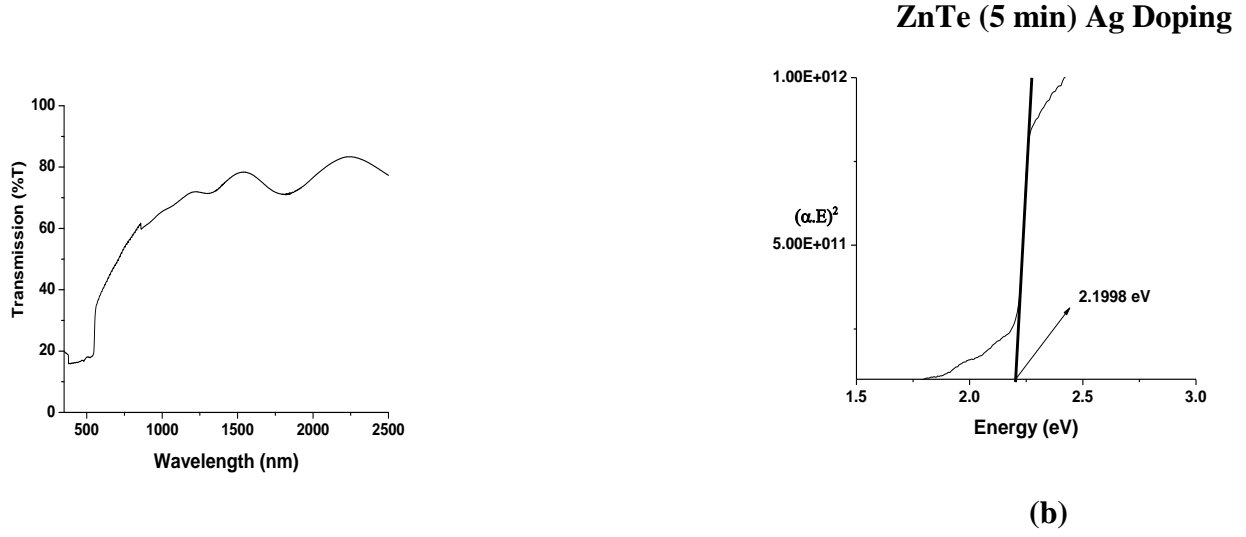
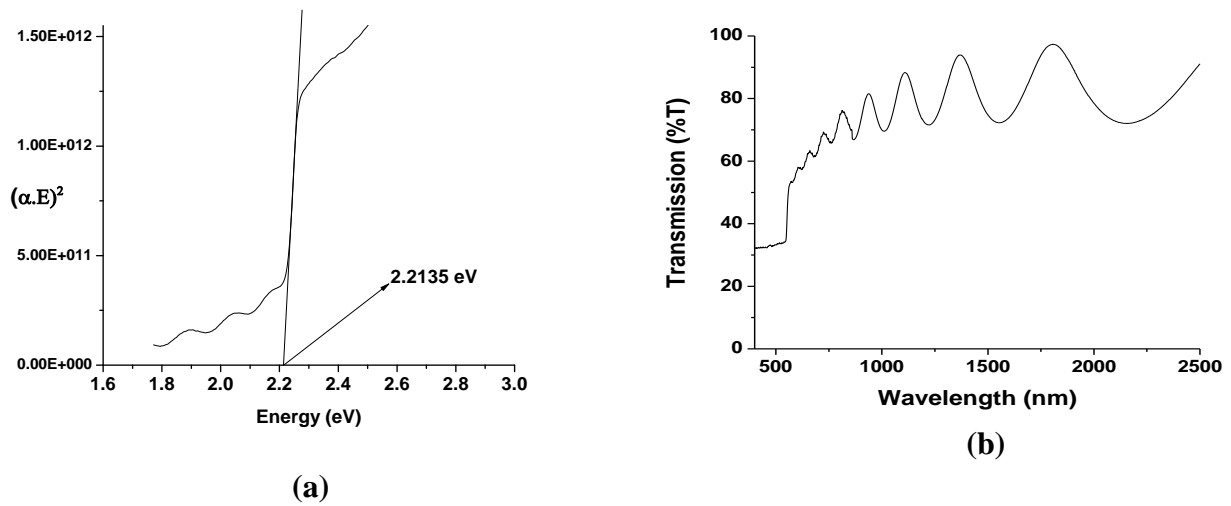


Figure 6. 7: (a,b) Optical band gap after annealing is 2.1998



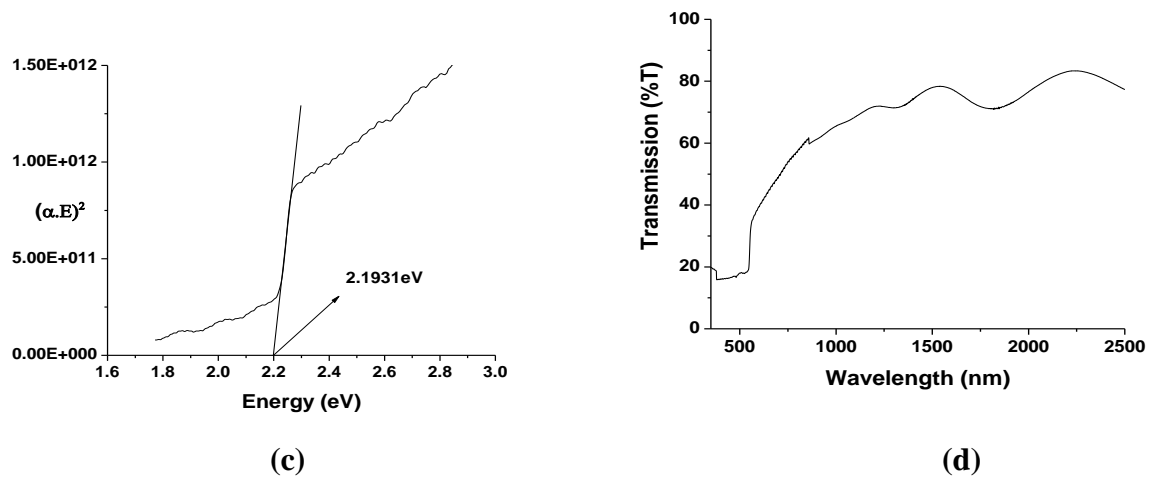


Figure 6. 8: (a-d): ZnTe Ag doped

Fig. 6.8 shows band gap and transmission of Ag doped samples for 10 and 15 min ZnTe samples. Results are compared on basis of Ag and Cu doping with ZnTe are shown in Fig 6.9-6.10.

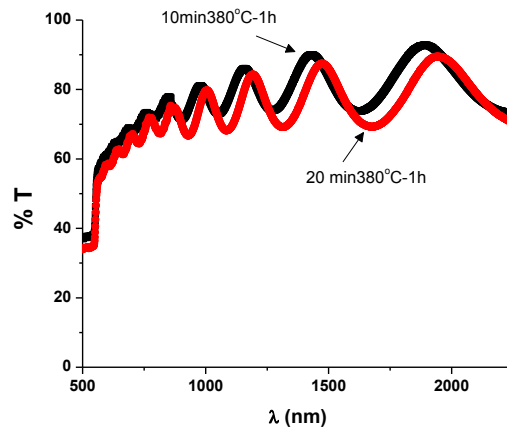


Figure 6. 9: Transmission behavior of Cu-doped ZnTe

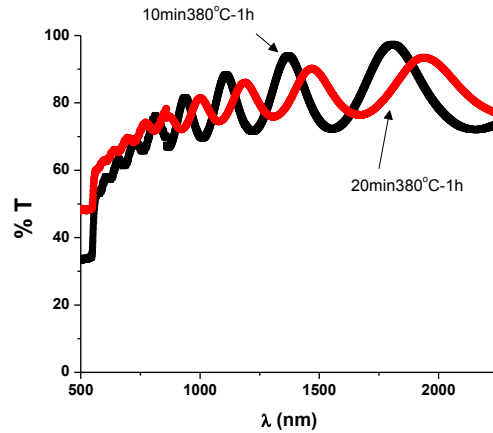


Figure 6. 10: Transmission behavior of Ag-doped ZnTe

Fig.6.9 shows the transmittance behavior of Cu-doped films at different evaporation times and Fig 6.10 shows the Ag-doped films at different evaporation times. It is clear that usual behavior (and also confirmed) [3] of decrease in transmittance is obvious with increase in evaporation time for the doped films.

In optical properties the transmission and band gap of these films changes as doping increases like transmission increases after annealing of as deposited samples and band gap decreases also after doping and annealing band gap gradually decreases as shown in table 6.1.

Table 6. 1: Optical Band Gaps of Ag Doped

Sample	Optical Band Gap (eV)
As Deposited	2.2384
Annealed	2.2332
5 min Doping	2.1998
10 min Doping	2.1931
20 min Doping	2.2122

Table 6. 2: Optical band Gaps of Cu Doped

<i>Sample</i>	<i>Optical Band Gap (eV)</i>
As Deposited	2.2384
Annealed	2.2332
5 min Doping	2.2040
10 min Doping	2.1998
20 min Doping	2.2111

It is observed that optical band gap of annealed films is almost remained same but with doping it decreases depending upon evaporation time. For small evaporation time there is small decrease in band gap has been observed.

6.5 Variation in Refractive Index

Slightly increase in refractive index was observed before and after doping and this also increased by increasing evaporation times. This is also reported in the previous work [4]

Refractive indices for as deposited, annealed and doped samples are shown in the table below.

Table 6.3 showing refractive indices

Refractive Indices for Cu Doped

Refractive Indices for Ag Doped

As deposited	2.27618	As deposited	2.27618
Annealed	2.3286	Annealed	2.3286
5 (minutes)	2.2673	5 (minutes)	2.29076
10 (minutes)	2.30047	10 (minutes)	2.30368
20 (minutes)	2.3067	20 (minutes)	2.3147

References:

- [1] V.S. John, Solid-State Electronics 49 (2005) 3–7
- [2] Akram K.S.Aqili, et al, applied surface science, 167 2000. (1–11)
- [3] Akram K.S.Aqili, et al, applied surface science, 180, 2001 (73-80)
- [4] Akram K.S.Aqili, et al Applied Surface Science, 191 (2002), 280-285

Conclusions

ZnTe films were fabricated on glass substrate by Close Space Sublimation (CSS) technique successfully. The films were annealed at 300°C and doped with Ag and Cu. X-Ray diffraction pattern confirmed the structural aspects. Scanning electron microscopy (SEM) was used to investigate the microstructure and morphology which was also examined with AFM.

Optical characterizations were carried out by Spectrophotometer for as deposited, annealed and doped samples varying in evaporation times at each soaking temperature. The thickness of films was calculated from Spectrophotometer data along with band gap refractive index and transmission. In optical properties the transmission and band gap of these films changes as doping increases and transmission also increases after annealing of as deposited samples and band gap decreases i.e. because of doped with metallic elements. Also after doping and annealing, band gap gradually decreases. Electrical measurements shows films are p-type semiconductor and their nobilities/conductivities are in close agreement with reported data in literature for ZnTe films. The major purpose of this work was fabrication of ZnTe doped and undoped thin films and their effect on optical and electrical properties. Both of these properties were enhanced with annealing and as well with doping. The decrease in electrical resistivity was observed with annealing and as well as with doping. It was observed that the maximum electrical resistivity was decreased in case of Cu doping. Furthermore, the optical properties such as band gap were influenced with dopant concentration, time and dopant type. The minimum band gap was observed for Cu dopant. It was observed that with increase in doping time the optical band gap of deposited film decreases. This decrease in optical band gap leads to improve the optical properties because the valance bands come closer to conduction band enhances the optoelectronic efficiency of material. In our case, we have improved the electrical properties of ZnTe film by doping. The minimum resistivity ($6.43 \times 10^{+1} \Omega\text{-cm}$) was observed for Cu doped ZnTe for 20 minutes. The decrease in resistivity values with dopant contribute in improvement of optical properties.

Future work

In future, work we have planned to fabricate more efficient solar cell based on CdTe/CdS thin films using CSS, chemical bath deposition (CBD), spin coating techniques etc. The film thickness strongly influences optical properties. We have also planned to produce ultra-thin film hetero junction based solar cells.